The Four Plutonic Belts of the Transhimalaya-Himalaya: a Chemical, Mineralogical, Isotopic, and Chronological Synthesis along a Tibet-Nepal Section

by FRANÇOIS DEBON, PATRICK LE FORT, SIMON M. F. SHEPPARD AND JACQUES SONET

Centre de Recherches Pétrographiques et Géochimiques (C.R.P.G.), B.P. 20, 54501 Vandoeuvre-lès-Nancy, France

(*Received 24 July 1984; revised typescript accepted 5 July 1985*)

ABSTRACT

The geochemistry (major, trace element, O- and Sr-isotope ratios) and petrology of the Transhimalaya, North Himalaya, High Himalaya and 'Lesser Himalaya' plutonic belts are compared based on the analyses of up to 492 samples.

The composite Transhimalaya batholith is subalkaline or monzonitic in character rather than calc-alkaline. Its genesis was probably closely related to subduction processes associated with strike-slip movement. It was emplaced on both sides of the boundary between an earlier metavolcanic arc and a continental margin. Two principal periods of magmatic activity occurred: Upper Cretaceous and, particularly in this region, Eocene at the time of the India-Eurasia collision when sediments may have become involved in the subduction process. Magmatic differentiation, characterized by two superimposed stages of evolution, and hybridization processes, involving both basic and acidic magmas, can account for the genesis of the different plutonic units. Although a continental contribution is implied, the isotopic data ($6{\cdot}8 < \delta^{18}O < 9{\cdot}2$; $0{\cdot}704 < {}^{87}Sr/{}^{86}Sr_i < 0{\cdot}707$) preclude a significant contribution from either old crust or surface derived sediments.

The North, High and 'Lesser' Himalaya plutonic belts are fundamentally different and correspond to aluminous associations of two groups of ages (Lower Palaeozoic for the 'Lesser Himalaya' and part of the North Himalaya; Upper Cenozoic for the High Himalaya and part of the North Himalaya). They are all high-$\delta^{18}O$ ($9 < \delta^{18}O < 14$) granites and adamellites with high initial ${}^{87}Sr/{}^{86}Sr$ ratios ($0{\cdot}709$ to $> 0{\cdot}740$). The Lower Palaeozoic group was generated within the Gondwana continental crust, independent of any true orogenesis, with a probable but limited contribution from the mantle. High Himalaya and North Himalaya Cenozoic plutons are directly linked to the activity of the Main Central Thrust. They were derived by similar anatectic processes of the same continental source rocks. The small but distinct chemical and mineralogical differences among the plutons are related to the increase in the intensity of anatexis on going towards the north and the east.

INTRODUCTION

Four continental-scale plutonic belts occur in the Nepal-South Tibet region (Fig. 1). From north to south the belts are: (1) the Transhimalaya or Kangdese, (2) the North Himalaya or Lhagoi Kangri, (3) the High Himalaya, and (4) the 'Lesser Himalaya'. The Transhimalaya belt lies just to the north of the Indus-Tsangpo suture zone (Fig. 2). It is characterized by a huge quasi-continuous 2600 km long batholith with rocks ranging from gabbro to granite. The three other belts are mainly composed of two-mica adamellites and granites. The North Himalaya belt runs some 50 km to the south of the suture zone. It forms a series of oval shaped domes up to a few tens of kilometres across. The High Himalaya belt is composed of a

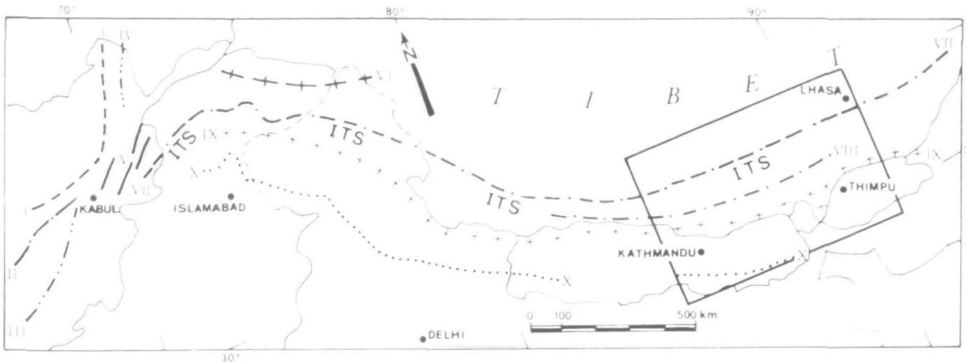

FIG. 1. The ten principal plutonic belts in the India–Eurasia suture zone. For I to VI see Debon *et al.* (1981); VII Transhimalaya (or Kangdese), VIII North Himalaya (or Lhagoi Kangri); IX High Himalaya; X 'Lesser Himalaya' The rectangular area corresponds to Fig. 2. The Indus–Tsangpo suture (ITS) lies south of the Transhimalaya (VII)

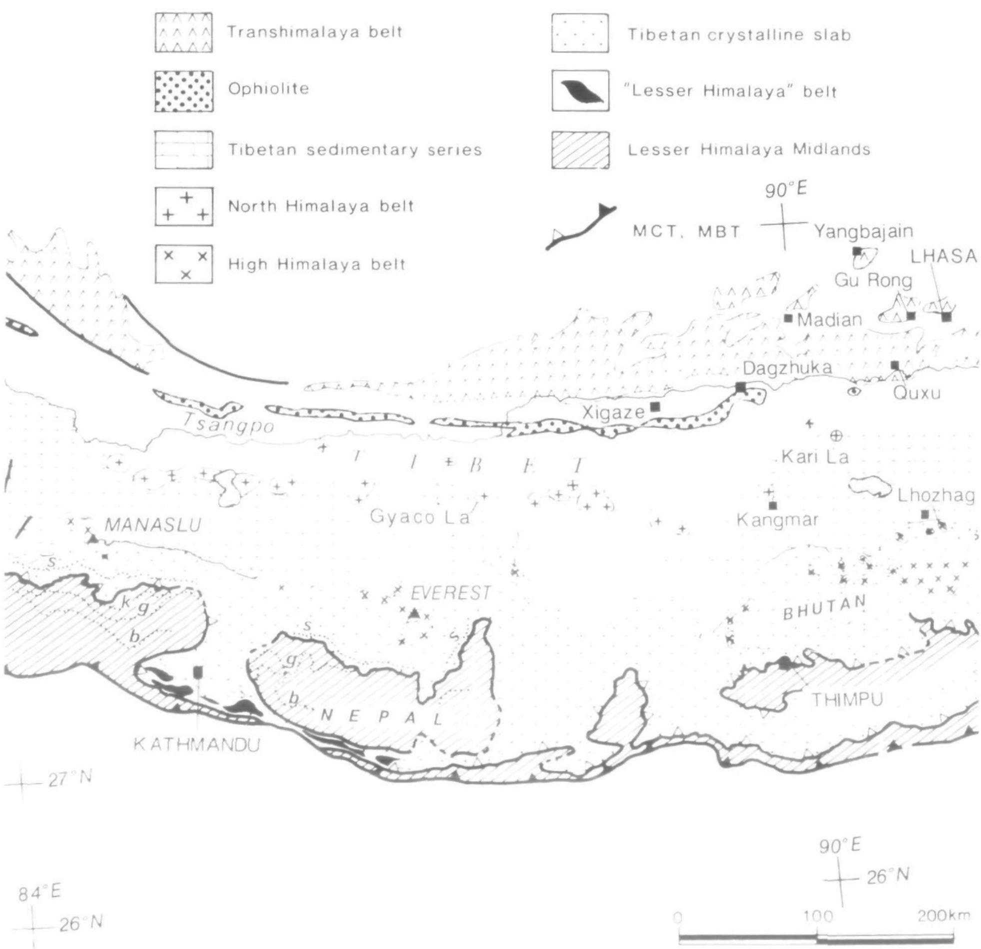

FIG. 2. Sketch map of the main structural divisions of Himalaya–Transhimalaya and of the four plutonic belts studied in the Nepal-Bhutan-Southern Tibet area (modified after Fig. 1 in Le Fort, 1983). The northern boundary of the Tibetan sedimentary series with the Indus-Tsangpo flyschoid and mélange series is not well known and tectonically complex. Letters for the metamorphic isograds (dotted lines) in Nepal are: b = biotite, g = garnet, k = kyanite and s = sillimanite. Abbreviations MCT = Main Central Thrust, MBT = Main Boundary Thrust.

number of irregularly spaced plutons of leucocratic rocks emplaced into the Tibetan sedimentary series to the north and above the Main Central Thrust (MCT). The 'Lesser Himalaya' is a discontinuous belt composed of both gneissic and non-gneissic granites which in general appears a short distance north of the Main Boundary Thrust (MBT) in the overthrust slab of the MCT.

This paper presents the petrology and geochemistry of 22 plutonic units from parts of these four belts. The region studied (Fig. 2) covers some 180000 km^2 and includes areas only recently open to geological investigations. The study is based on the chemical, isotopic, mineralogical, and petrological analysis of up to 492 samples. The rock types are precisely defined and the petrochemical characteristics of the individual belts are determined using a chemical-mineralogical analysis (Debon & Le Fort, 1982). The magmatic associations thus characterized are then related to the evolution of the Gondwana or Indian plate, the northward subduction of the Tethys floor, and the final collision between the Indian and Eurasian plates.

ANALYTICAL METHODS

Major (SiO_2, Al_2O_3, total iron as Fe_2O_3, MnO, MgO, CaO, Na_2O, K_2O, TiO_2, P_2O_5) and some trace elements (Ba, Rb, Sr) of whole rock samples (Tables 1, 3, 5) were determined at C.R.P.G. (Govindaraju *et al.*, 1976). The acid-dissolved, lithium borate fusion melts of the silicate samples were analysed using a direct-reading optical emission spectrometer (ARL 31000) equipped with a microwave plasma excitation source. The analysed solutions are buffered with Sr in order to eliminate matrix influences. International geochemical standards were used systematically for the construction of calibration curves. Loss on ignition was measured before fusion on 1 g of sample ignited for some 15 hours at 1000 °C using an electric muffle furnace.

The REE (La, Ce, Nd, Sm, Eu, Gd, Dy, Er, Yb, Lu) and Y contents of selected rock samples (Table 4) were determined on an emission spectrometer (JY 48 P) equipped with an inductively coupled plasma source (ICP) (Govindaraju & Mevelle, 1983). Before analysis the REE were separated using a robotic system (Lab Rob JY 308). The lower limit of determination is down to one or two times chondrite level(s) for most elements.

Oxygen isotopes on whole rock samples (Table 5) were analysed using a modification of the BrF_5 technique (Clayton & Mayeda, 1963). The $^{18}O/^{16}O$ ratios are expressed as $\delta^{18}O$ relative to SMOW in per mil with a reproducibility of better than $\pm 0{\cdot}2$ per mil on duplicate analyses. The value for NBS-28 is 9·60.

Rb-Sr isotope analyses (Table 7) were determined by mass spectrometry. The relative error for the $^{87}Rb/^{86}Sr$ ratios is less than 2 per cent. The $^{87}Sr/^{86}Sr$ ratios were determined using one of the two mass spectrometers: (i) Thomson 206 S for units with an adequate variation in $^{87}Rb/^{86}Sr$ ratio. The error (2σ) for a duplicate run is less than 0·0001. The value for NBS 987 is $0{\cdot}71025 \pm 0{\cdot}0001$. (ii) Cameca 206 SA new generation for units with a small variation in $^{87}Rb/^{86}Sr$ ratio. The error (2σ) for a duplicate run is less than 0·00005. Value for NBS 987 is $0{\cdot}710199 \pm 0{\cdot}000025$. The analytical error for each sample is given in Table 7. $\lambda^{87}Rb = 1{\cdot}42 \times 10^{-11}\ a^{-1}$.

BULK CHEMICAL VARIATIONS

The major element chemical data from Table 3 are presented on an AFM diagram (Fig. 3). The fields for the individual belts describe trends which are typical of very many other intrusive provinces. Independent of the geological arguments, the overlapping of the fields for the four belts does not imply that the different rocks are related to a common parent magma

(Le Maître, 1976). Despite the wide use of such diagrams to discuss plutonic provinces (e.g. Atherton *et al.*, 1979), the diagram is not very discriminating. For example many relatively small differences in major element composition which are considered to reflect important petrogenetic differences are not resolved in this diagram. Similarly the role of alumina in granitoids which plot near the alkali pole, such as many of our samples, cannot be appreciated. Other widely used diagrams such as Harker diagrams are equally unhelpful in aiding the interpretation of such series of chemical data.

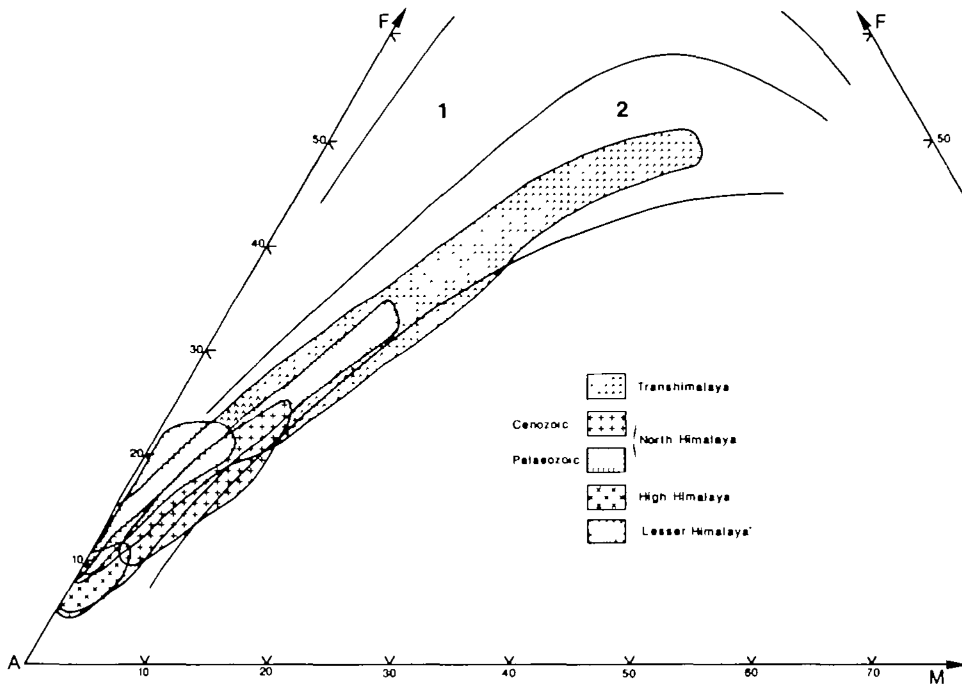

FIG. 3. Compositional characteristics (data from Table 3) of the four plutonic belts in the AFM diagram ($A = Na_2O + K_2O$, F = total iron as FeO, M = MgO). The domains 1 and 2 correspond to pigeonitic (tholeiitic) and hypersthenic (calc-alkaline) series of Kuno (1968) respectively. Although this diagram suggests that these plutonic associations are calc-alkaline, most of Transhimalaya are subalkaline or monzonitic and the North, High and 'Lesser' Himalaya are aluminous (see text for discussion).

More serious than these limitations however is the often misleading character of the diagram. For example, the majority of our data plot within the general field of calc-alkali rocks (Fig. 3) despite the fact that they are not actually calc-alkaline (see below). Recently some methods have been developed to avoid such misinterpretations and to reveal more clearly differences among individual associations (La Roche, 1964, 1980; Chappel & White, 1974; La Roche *et al.*, 1980; Debon & Le Fort, 1982). In particular the chemical-mineralogical method of analysis of Debon & Le Fort (1982) is applied here (Figs. 4, 5, 6) for a number of reasons. The method is based on quantitative chemical analyses of major elements in preference to modal microscopic data with their more limited reproducibility. The relationships between variations in mineralogy and chemistry are emphasized and it gives a rigorous definition of the typology both of igneous rock samples (nomenclature, characteristics) and of their magmatic associations. The method is applicable to most of the common igneous rocks from gabbros to syenites to leucocratic muscovite granites. It is

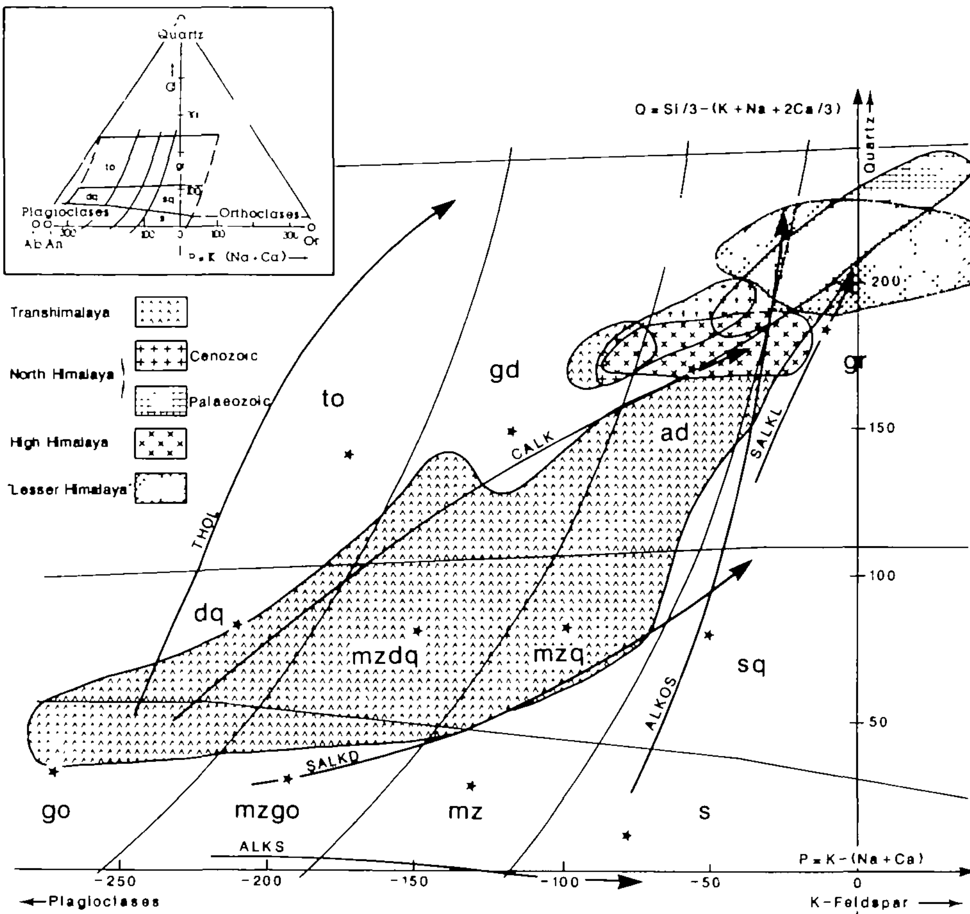

FIG. 4 Distribution of the four plutonic belts in the 'nomenclature' diagram proposed by Debon & Le Fort (1982) after La Roche (1964, 1966) and Streckeisen (1976). The two parameters are in gram-atoms × 10^3 in 100 g of rock or mineral. Each field corresponds to a petrographic type: gr granite, ad adamellite, gd granodiorite, to tonalite, sq quartz syenite, mzq quartz monzonite, mzdq quartz monzodiorite, dq quartz diorite, s syenite, mz monzonite, mzgo monzogabbro, go gabbro. The reference system of mean compositions corresponding to each of these types is shown by black stars. For comparison, typical trends of different subtypes of cafemic or alumino-cafemic associations (Fig. 5) are shown: THOL tholeiitic, CALK calc-alkaline, SALKD, SALKL dark and light-coloured subalkaline (i.e. monzonitic) respectively, ALKS, ALKOS alkaline saturated and oversaturated respectively. The plutonic units included in each belt with number of analysed samples (n) are all those given in Table 3.

equally applicable to volcanic rocks (basalts, trachytes, etc.). The rock classification and nomenclature used here is in general agreement with terminology based either on mineralogical (e.g. Streckeisen, 1976) or chemical parameters.

THE TRANSHIMALAYA (OR KANGDESE) BATHOLITHIC BELT

The batholith in Southern Tibet (Fig. 2) is composed of a main composite body (or batholith *sensu stricto*) associated with a swarm of isolated plutons along its northern edge. Two transverse sections of the batholith *s.st.* (Quxu and Dagzhuka) were studied and four of the northern plutons (Madian, Yangbajain, Gu Rong, Lhasa).

In our area, the batholith intrudes metasediments and metavolcanics of Palaeozoic and

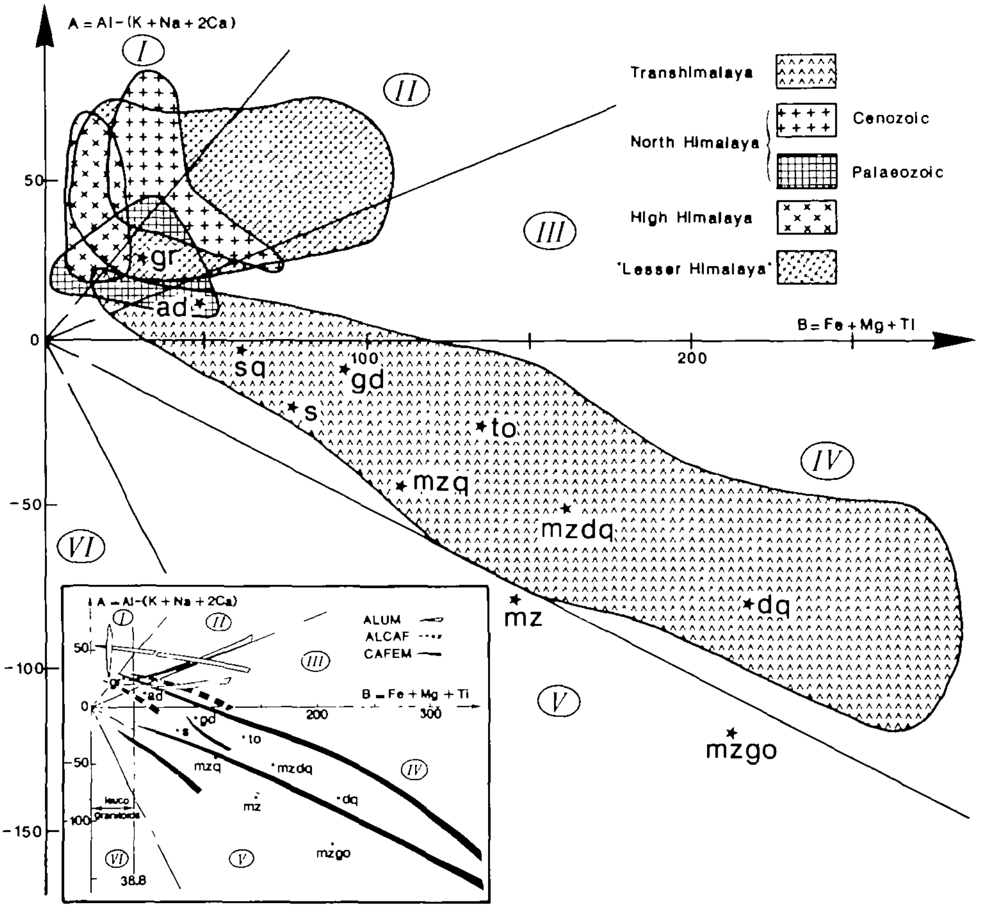

FIG. 5. Distribution of the four plutonic belts in the 'characteristic minerals' diagram of Debon & Le Fort (1982). The parameters are in gram-atoms × 10^3 in 100 g of rock or mineral; A is the 'aluminous index' and B is proportional to the dark mineral content (La Roche, 1964). This diagram separates peraluminous rocks or minerals with positive value of A, e.g. biotite (Bi), muscovite (Mu), from metaluminous ones, e.g. amphibole (Amph), clinopyroxene (Cpx). Each of its six sectors, numbered from *I* to *VI*, corresponds to a specific mineralogical composition; to a first approximation: *I* rocks with Mu > Bi (by volume), *II* Bi > Mu, *III* Bi, *IV* Bi + Amph ± Cpx, *V* Cpx ± Amph ± Bi. The trends of the three main types of magmatic associations (see the inset) are distinguished: ALUM aluminous, ALCAF alumino-cafemic, CAFEM cafemic. See Fig 4 for other explanations.

Mesozoic ages (e.g. Academia Sinica, 1980; Jin, 1981; Burg, 1983). In the vicinity of Quxu village (Fig. 7), it intrudes a thick metavolcanic (amphibolitic) formation of assumed ophiolitic character (Proust *et al.*, 1984) and Triassic age (e.g. Burg, 1983). This formation includes rocks of basaltic, quartz andesitic and dacitic compositions (Table 1) and corresponds to a cafemic tholeiitic association. The abundance of intermediate rocks (54–60 per cent of SiO_2 on average; Table 1) and the low TiO_2 contents (0·7–0·8 per cent on average) suggest that it formed in an island-arc environment. It can be compared with the Upper Jurassic to Upper Cretaceous Dras Volcanic arc in Ladakh (Reibel & Juteau, 1981; Honegger *et al.*, 1982; Dietrich *et al.*, 1983). Based on some forty whole rock chemical analyses (unpublished data), there is probably no typical calc-alkaline volcanism in our area in contrast to other opinions (e.g. Coulon & Wang Songchan, 1983). Most of the Cretaceous and Paleogene volcanic associations are subalkaline (i.e. latitic).

TABLE 1

Mean chemical compositions of Quxu metavolcanics

Rock type	*n*	SiO_2	Al_2O_3	Fe_2O_3*	MnO	MgO	CaO	Na_2O	K_2O	TiO_2	P_2O_5	L.I	*Total*	Ba	Rb	Sr
Metabasalts	3	50·90	16·14	8·10	0·17	8·23	8·99	4·02	0·41	0·76	0·36	1·68	99·56	65	3–10	303
Metaquartz andesites	4	54·14	16·42	8·64	0·17	5·19	9·09	2·71	0·98	0·72	0·24	1·33	99 63	215	15	516
Metadacites	5	60·17	15·57	6·97	0·11	3·45	6·67	3·49	0·73	0·71	0·21	1·55	99·63	105	11–15	400

n number of analysed samples.
* total Fe as Fe_2O_3.
L.I. loss on ignition.
Trace elements in p.p.m.

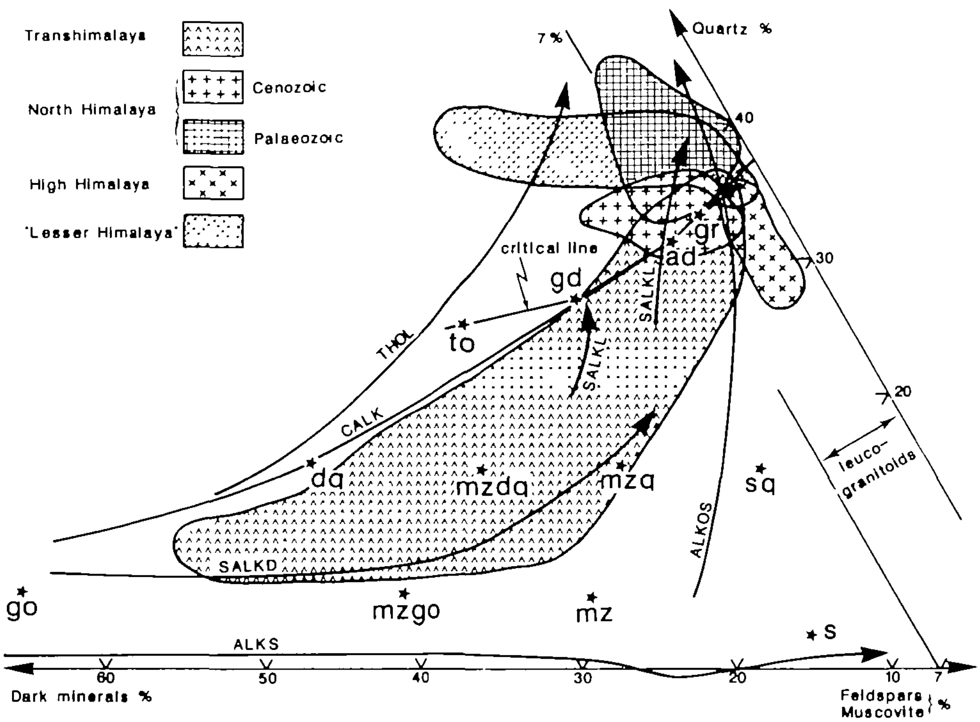

FIG. 6. Distribution of the four plutonic belts in the triangular quartz–dark minerals–feldspar + muscovite diagram ('Q–B–F' diagram). The parameters in weight percent are directly calculated from chemical analyses (La Roche, 1964; Debon & Le Fort, 1982). The different subtypes among the three main types (Fig. 5) of magmatic associations are distinguished: THOL, CALK, SALKD, SALKL, ALKS, ALKOS among the cafemic or alumino-cafemic associations (typical trends are shown for comparison); quartz-rich, quartz-normal and quartz-poor subtypes among the aluminous associations (according to the positions of their plots above, on, or below the 'critical line'). Other explanations as in Fig. 4.

Petrographical and geochemical characteristics

Like most batholiths (e.g. Pitcher, 1978), the Transhimalaya is composite. It is made up of numerous contiguous or isolated, but associated, plutonic bodies (Academia Sinica, 1980; Tu *et al.*, 1981, 1982; Debon *et al.*, 1982, 1984; Brun *et al.*, 1983; Zhou & Jin, 1983; Jin & Xu, 1984; Liu, 1984). Along the Quxu section (Fig. 7), four major plutonic units, named A (divided into A1 and A2), B, C, and D, have been distinguished on the basis of both field and chemical criteria (Debon *et al.*, 1982, 1984; Tables 2, 3; Figs. 10, 11). The boundaries between adjacent units are generally gradational, suggesting that the units were emplaced simultaneously. However, the contacts of A1 and D with the other units have not been observed. Along the Dagzhuka section (Figs. 2, 11), two major units, named the South Tsangpo and the North Tsangpo units (south and north bank of the river respectively), occur. The northern half of the batholith is very heterogeneous here and rich in metasedimentary and metavolcanic septa. The northern plutons are similarly composite, except Yangbajain; they are made up of two or three chemically distinct zones (Debon *et al.*, 1982, 1984; Tables 2, 3).

Plutonic units of the Quxu section display a well developed foliation with all stages between a planar flow structure and, particularly in the D unit, a post-magmatic schistosity with partial recrystallization (Fig. 7). In addition, except in A1, dark igneous 'microgranular' rocks (Didier, 1973) are very abundant (up to some 20 per cent by volume). These rocks occur either as pseudo-dykes or, more commonly, as isolated decimetric lenses lying along the

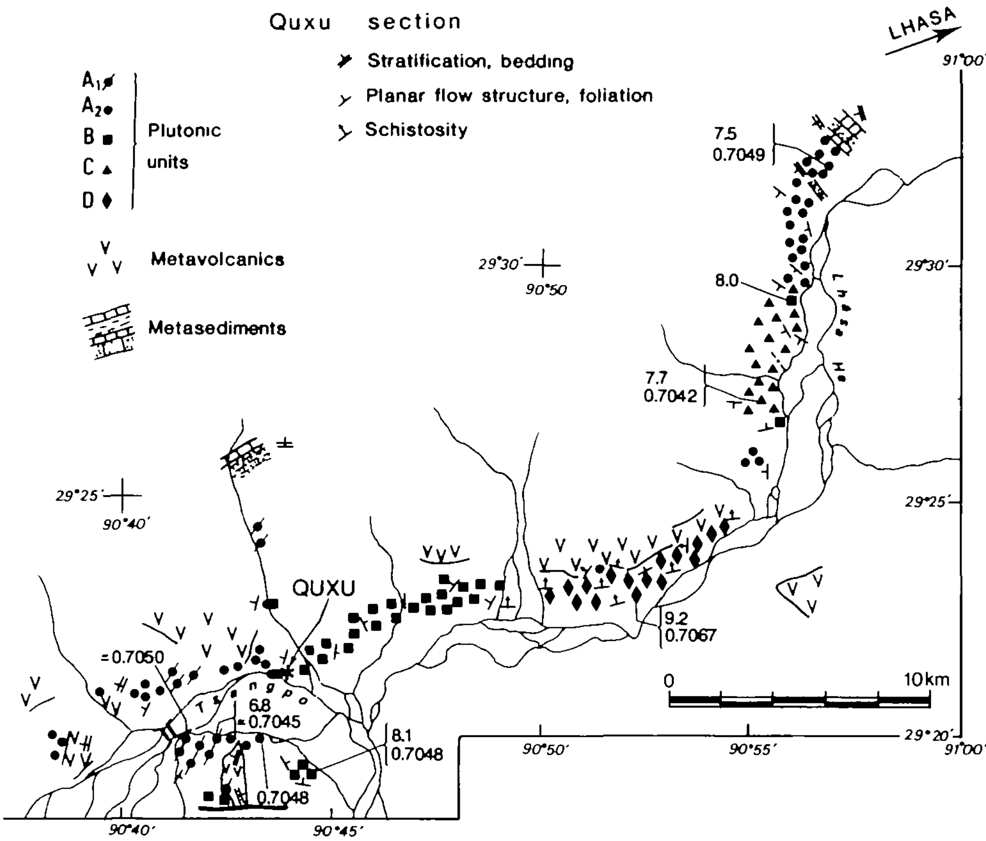

FIG. 7. Sketch map of the Transhimalaya batholith *s.st.* along the Quxu section (or Quxu super-unit), south-west of Lhasa, with $\delta^{18}O$ values and initial strontium isotope ratios (Tables 5, 6, 7). The metavolcanics are amphibolites

foliation. In either form, they always appear to have been emplaced under magmatic conditions.

The batholith is composed of a wide range of petrographic types (Fig. 4) including in decreasing order of importance (Table 3), adamellites, quartz monzodiorites, granodiorites and, to a lesser extent, gabbros, quartz diorites, granites, quartz monzonites and monzonites. Their relative abundance, however, may vary greatly from one plutonic unit to another (Tables 2, 3). Most rocks are metaluminous (Fig. 5, Table 3). Relative to the reference compositions of Debon & Le Fort (1982), they are in general normal or rich in feldspars, alkalis (sum Na + K) and Ba, normal or poor in quartz and dark minerals, Sr-rich but Rb-poor; in addition, they have low loss on ignition and their Mg/Fe ratios are usually normal or high (Table 3).

These rocks are principally composed of quartz; K-feldspar, fairly often with the microcline twinning but usually without much perthite; concentrically-zoned plagioclase, sometimes with patchy zoning but generally with a core of andesine and a rim of oligoclase or andesine; biotite with Mg/(Fe + Mg) ratios from 0·45 to 0·61; amphibole, usually magnesio-hornblende; orthopyroxene which is restricted to gabbros; clinopyroxene as isolated crystals in gabbros and sometimes as relics elsewhere; often abundant very titanium-poor oxides (magnetite or hematite); rare ilmenite; frequent sphene.

The REE contents and patterns (Table 4, Fig. 8) are quite comparable to those of both

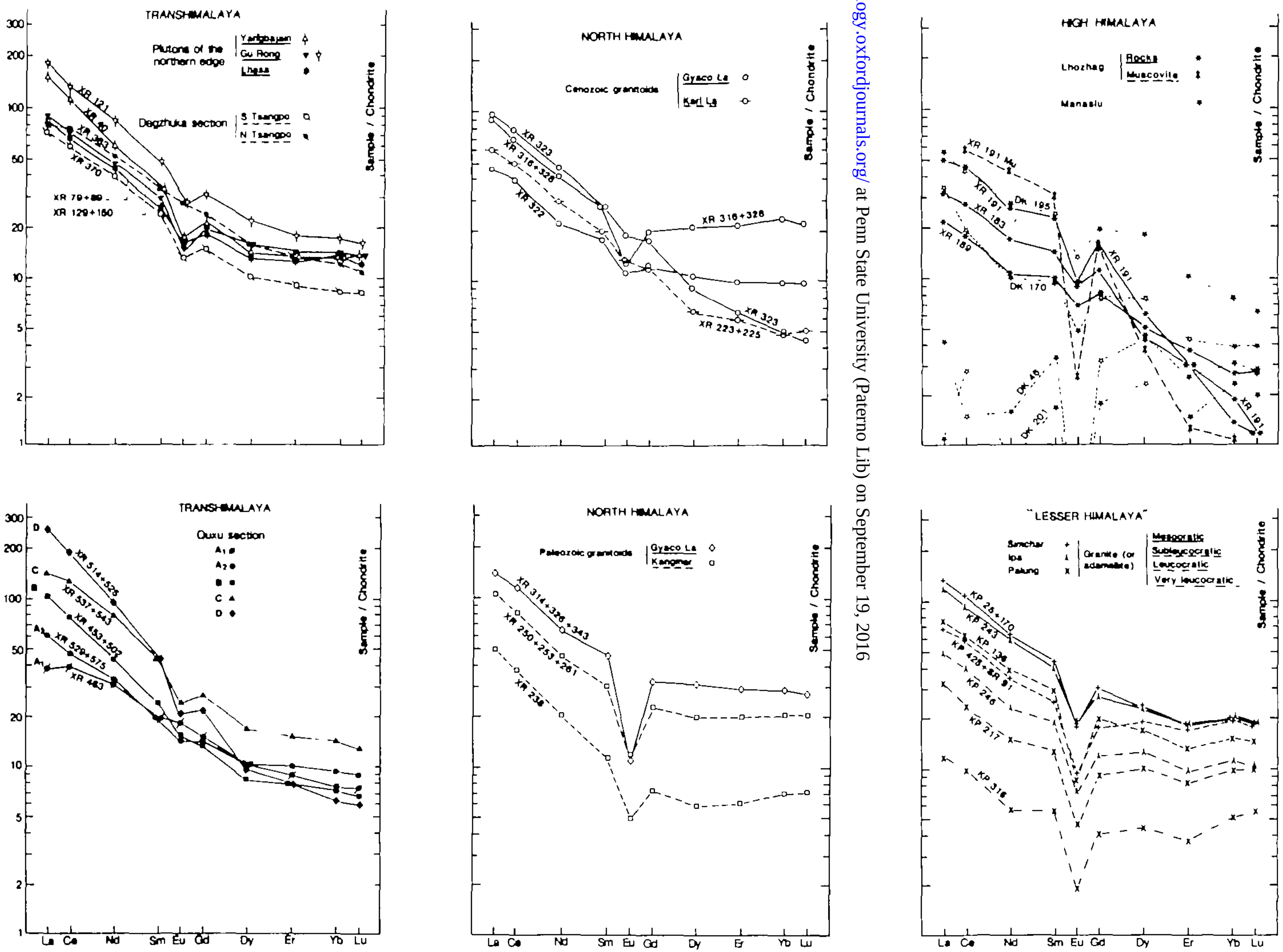

FIG. 8. REE patterns of selected samples. The data (Table 4) are normalized to chondritic values given by Evensen *et al* (1978)

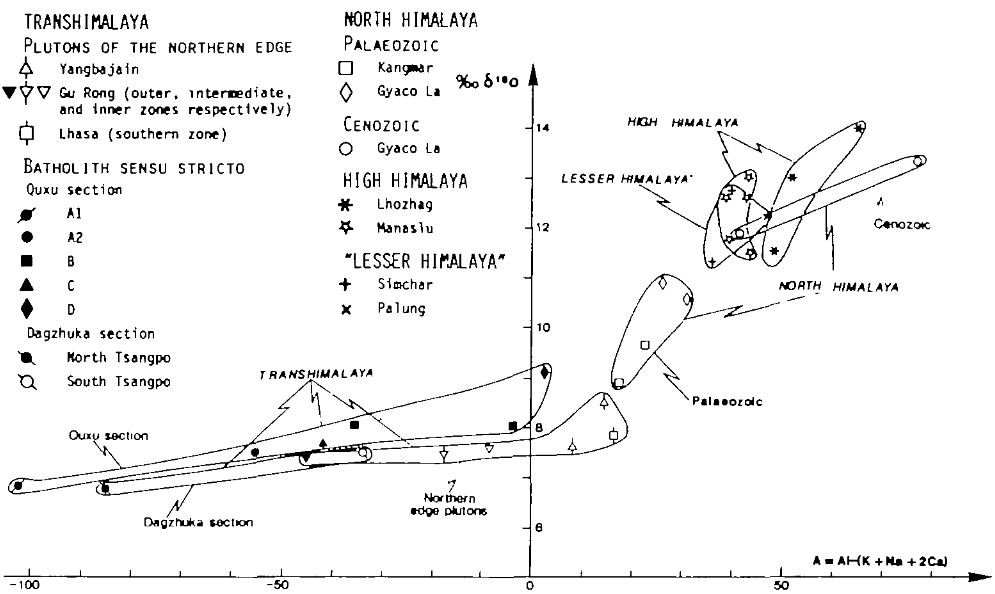

FIG. 9. $\delta^{18}O$ (Table 5) *vs.* 'aluminous index' (Fig. 5) for selected samples from the four plutonic belts.

subalkaline (i.e. monzonitic) and calc-alkaline granitoids (e.g. Atherton *et al.*, 1979; Fourcade, 1981; Fourcade & Allègre, 1981). For the Quxu section, the REE patterns display a progressive enrichment in light-REE from A1 to D through A2, B and C, confirming the distinction based on major elements between (A1 + A2), B, C and D, the relationship of A1 with A2, and the increase of the monzonitic character from (A1 + A2) to D (e.g. Fig. 10). Similarly, these patterns support a close relationship between the outer and the inner zones of the Gu Rong pluton and distinguish these two zones from the intermediate one.

The oxygen isotope composition of the batholith is relatively homogeneous with $\delta^{18}O$ values ranging from 6·8 to 8·5 per mil (one value at 9·2) (Sheppard *et al.*, 1983 and new data; Table 5). Based on hydrogen isotope analyses (unpublished data) there is no evidence that the rocks may have been modified by convective circulation of meteoric waters during their post-magmatic history. The $\delta^{18}O$ values are therefore considered to record their magmatic signature. In each of the three studied areas (Quxu and Dagzhuka sections, northern plutons) the $\delta^{18}O$ values increase slightly and regularly with increase in the 'aluminous index' (Fig. 9). There is a slight negative correlation with increase in dark mineral content. These rocks are thus in the I and H_1 groups of Taylor (1968). They are therefore depleted in $\delta^{18}O$ relative to most of the large batholithic masses previously analysed.

The northern plutons as well as the plutonic units of the batholith *s.st.* correspond to distinct magmatic associations (Figs. 10, 11; Debon *et al.*, 1982, 1984), the typology of which is summarized in Table 2. They are cafemic or alumino-cafemic associations (Fig. 5) and most of them are either typically subalkaline (i.e. monzonitic) or transitional between the subalkaline and the calc-alkaline types (Figs. 4, 6, 10). Similar to the volcanics occurring in this area and contrary to widely accepted opinion (e.g. Maluski *et al.*, 1982; Schärer *et al.*, 1984*b*) there are no strictly calc-alkaline associations in this part of the Transhimalaya batholith; subalkaline trends are dominant (Fig. 6). The presence of quartz monzodiorites, quartz monzonites and monzonites, the complete lack of tonalites (Fig. 4), and the mineralogical features such as the relatively low dark mineral content and high abundance of feldspars and sphene support this conclusion.

TABLE 2

Typology of the Transhimalaya plutonic bodies

	Super-unit	*Unit (or zone)*	*Main rock type*[1]	*Type & Subtype of association*		*Remarks*
PLUTONS OF THE NORTHERN EDGE	Madian	dark light-c.	mzdq/IV gr/II	CAFEM	SALKC	Only studied from boulders/2 groups of rocks and maybe 2 zones/Chemical gap betw the 2 groups
	Yangbajain		ad/III	ALCAF	SALKL	Septa-rich heterogeneous areas in north. part/ Only one major unit.
	Gu Rong	extern. interm inner	mzdq/IV ad/IV ad/IV	CAFEM	Transit. betw. SALKC & CALK	Maybe concentrically-zoned/Extern zone, ≤ 0·6 km thick, with sharp contacts/Chemical gap betw. extern and other zones/Conspicuous chemical en echelon ordering/Most light-c zone = interm zone.
	Lhasa	north south	mzdq/IV gd/III	CAFEM	Idem	Sharp contact and chemical gap betw. the 2 zones/South. zone very predominant, locally with septa/North. zone ≤ 1 km thick
BATHOLITH *sensu stricto*	Quxu Section	A1	go/IV	CAFEM	Transit. betw SALKD & CALK	Two pyroxenes/Zoned plagioclase. An 58–44%
		A2	dq, gd/IV	CAFEM	Idem	
		B	mzdq, gd/IV	CAFEM	SALKL	B and C have similar mean compositions
		C	Idem	CAFEM	SALKL	Specific porphyritic texture/Sharp or gradational boundaries.
		D	mzq, ad/IV	CAFEM	SALKL	Schistosed.
	Dagzhuka Section	North Tsangpo	go, mzdq/IV	CAFEM	Transit. betw ALKS & SALKD	Biotite of cm size/Two pyroxenes in gabbros/ Includes a heterogeneous area of acid and basic plutonic rocks
		South Tsangpo	mzdq/IV	CAFEM	Transit. betw. SALK & CALK	

The typology refers to the classification of Debon & Le Fort (1982).

[1] Main rock type defined as in Table 3.

Abbreviations: betw between; extern. external; interm intermediate; light-c. light-coloured; north. northern; south. southern; transit. transitional; ALCAF alumino-cafemic; CAFEM cafemic; ALKS alkaline saturated, SALK subalkaline (i.e monzonitic) respectively dark (SALKD), light-coloured (SALKL), composite (SALKC); CALK calc-alkaline

According to several authors (Academia Sinica, 1980; Brun *et al.*, 1983), the batholith becomes more and more acidic on going from south to north. Our observations only partly support such a trend. In general, on going from the batholith *s.st.* to the plutons of its northern edge, there is a decrease of the dark microgranular inclusions, dark minerals and Sr contents, and an increase of the quartz and Rb contents, and of the Sr isotope initial ratio (Fig. 2; Tables 3, 6, 7). Moreover, within the batholith *s.st.*, the darkest rocks (gabbros) occur in the southern part. However, along the Quxu section, judging from both the location and the mean compositions of the plutonic units including the isotopic compositions (Fig. 7), the major evolutionary trend within the batholith *s.st.* is not from south to north but centripetal, being roughly symmetrical about the central D unit (Figs. 7, 10; Table 3).

Chronological data

Based on recent chronological data (Tables 6, 7), two groups of ages occur in this part of the Transhimalaya batholith. The oldest group, from 82 to 113 Ma, has a mean value of about 93 Ma (Upper Cretaceous). It characterizes both the North and South Tsangpo units of the Dagzhuka section. The youngest group varies from 40 to 60 Ma and averages about 50 Ma (Eocene). It includes all the plutonic units occurring along the 90 km long transverse section from Yangbajain to the South of Quxu (i.e. the Yangbajain, Gu Rong and Lhasa plutons, and the A1, A2, B, C and D units in the batholith *s.st.*) (Figs. 2, 7). Being based on a variety of dating methods (Tables 6, 7), these ages very likely correspond to emplacement ages.

The initial $^{87}Sr/^{86}Sr$ isotope ratios range from 0·7036 to 0·7071, with an average of 0·705 (Tables 6, 7). As a whole, the northern plutons have higher initial ratios than the batholith *s.st.*

Genesis of the Transhimalaya batholith

The genesis of the batholith is generally considered to be related to the northward subduction of the Tethys floor but its geodynamic location (island arc or active continental margin) is more questionable. The batholith intrudes both metavolcanics (Quxu amphibolites) of probable island-arc origin to the south and platform sedimentary series to the north. These intrusive characteristics support an emplacement on both sides of the boundary between an earlier island-arc and the southern edge of the continental 'Lhasa block'. Trommsdorff *et al.* (1982) and Schärer *et al.* (1984*a*) have proposed a similar model for the Ladakh area. Its chemical-mineralogical typology is quite compatible with a genesis related to oceanic subduction. More precisely, its subalkaline (monzonitic) tendency is interpreted to indicate that the subduction was not perpendicular to the axial direction of the batholith. A strike-slip movement is proposed, comparable to that for the Arghandab plutonic belt (number III in Fig. 1) in Afghanistan (Afzali *et al.*, 1979). Such movement tends to generate zones of tension in the overlying plate margin and thus to promote the genesis and/or the emplacement of alkaline or subalkaline magmas. According to Brun *et al.* (1983), sinistral wrenching occurred here during batholith emplacement (see also Burg, 1983; Mascle, 1985).

The numerous Cenozoic ages, close to 50 Ma, for the batholith and some of the associated volcanics (48·5 ± 1·5 Ma for a Lingzizong formation, north of the batholith; Montigny *in* Westphal *et al.*, 1982) suggest that a major (?) part of the eastern Transhimalaya magma was emplaced a short time before and during the beginning of the India–Eurasia collision. Collision in this part of the suture zone occurred during Lower Eocene times, around 50 Ma, based on a number of independent methods including paleomagnetism and magnetic anomalies (Besse *et al.*, 1984; Patriat & Achache, 1984). This magmatism, though directly related to subduction processes, could therefore be a good indicator of the time of collision (Xu *et al.*, 1985). It suggests, as in the Adrar des Iforas area of Mali (Bertrand & Davison, 1981), that the culmination of the emplacement processes was determined by the beginning of the collision event (Debon *et al.*, 1985). This Eocene magmatic stage was preceded around Dagzhuka by a Cretaceous magmatic emplacement, as in Ladakh (e.g. Brookfield & Reynolds, 1981; Honegger *et al.*, 1982). There is therefore no clear systematic migration of the magmatism along the batholith. The duration of its emplacement may have lasted several tens of millions of years in a relatively restricted area. Similarly, in the area studied, no systematic migration is observed along transverse sections of the batholith.

The following discussion of the geochemical data is generally applicable to all of the plutonic units. To aid the discussion, however, fields for only some of the plutons are presented on the figures. The chemical-mineralogical (Figs. 10, 11) and isotopic (Fig. 9) diagrams and the field data show that the individual plutonic units are distinct from each

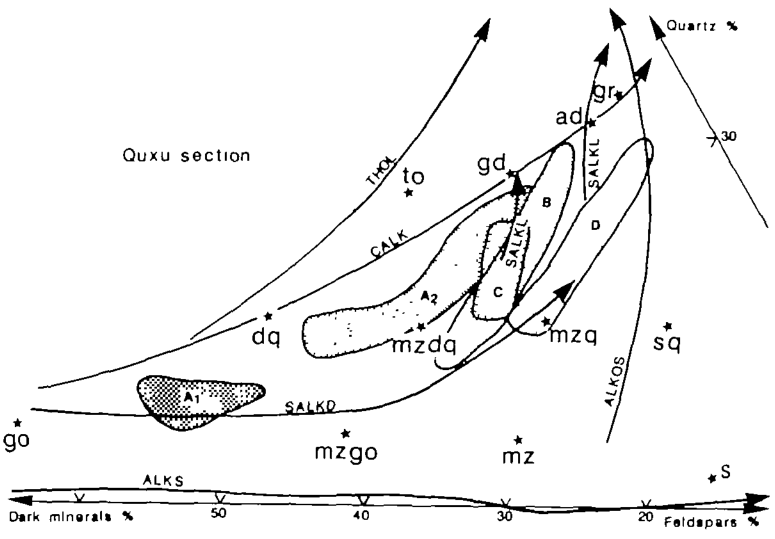

FIG. 10. Distribution of the plutonic units (A1, A2, B, C, D) of the Transhimalayan Quxu section (viz. of the Quxu super-unit; Fig. 7) in the triangular quartz-dark minerals-feldspar diagram. Other explanations as in Figs. 4 and 6.

other at their present level of emplacement. Nevertheless the form of the trends among the plutons are directly comparable. For example, on going from the darkest to the lightest members of each plutonic unit, the evolution follows classical trends of magmatic differentiation (Fig. 10). Similarly there is a regular decrease of the Mg/(Fe + Mg) ratio among the different units (Fig. 11). Figure 11 also shows that for a given value of (Fe + Mg + Ti) the ratio Mg/(Fe + Mg) tends to increase systematically on going from the darkest to the lightest coloured units of a group of associated plutons—in this case the Quxu and the Dagzhuka sections. Comparable systematics are seen in other diagrams (Figs. 8 to 11). These chemical similarities and differences and the coherent organisation of the fields among the different plutonic units implies that (1) plutonic units which are associated in the field form part of a genetically related group—the 'super-units' of Pitcher (1978) (Table 2), and (2) part of the evolution of each unit was more or less independent of other units. The evolution of a super-unit appears to be controlled by two superimposed stages of differentiation, well shown in chemical diagrams by the remarkable en echelon ordering of the different units (Figs. 10, 11). The earlier process, responsible for the dissociation of a super-unit into several units, could involve a common differentiation and/or hybridization event in a system of rather uniform initial Sr isotope ratio (Table 7) and presumably at depth, followed by individual and independent differentiation processes among each unit (Figs. 10, 11; Table 2). The exact processes have yet to be elucidated. Such a two-stage development appears particularly conspicuous in subalkaline or alkaline igneous complexes (e.g. Ballons massif in the Vosges; Pagel & Leterrier, 1980).

The precise nature of the source material(s) remains uncertain. The predominantly adamellitic, quartz monzodioritic and granodioritic composition of the batholith suggests the involvement of sialic crust. This is supported by the negative ε_{Nd} values (Gariepy *et al.*, 1983). The existence of gabbros (A1 and North Tsangpo units) and the locally very abundant dark microgranular inclusions suggest that there is a basic contribution which could possibly be of mantle origin (e.g. Leterrier & Debon, 1978). Both $\delta^{18}O$ and initial $^{87}Sr/^{86}Sr$ values are low (at about $7 \cdot 6 \pm 0 \cdot 8$ per mil and $0 \cdot 7050 \pm 15$ respectively) but higher than primary mantle

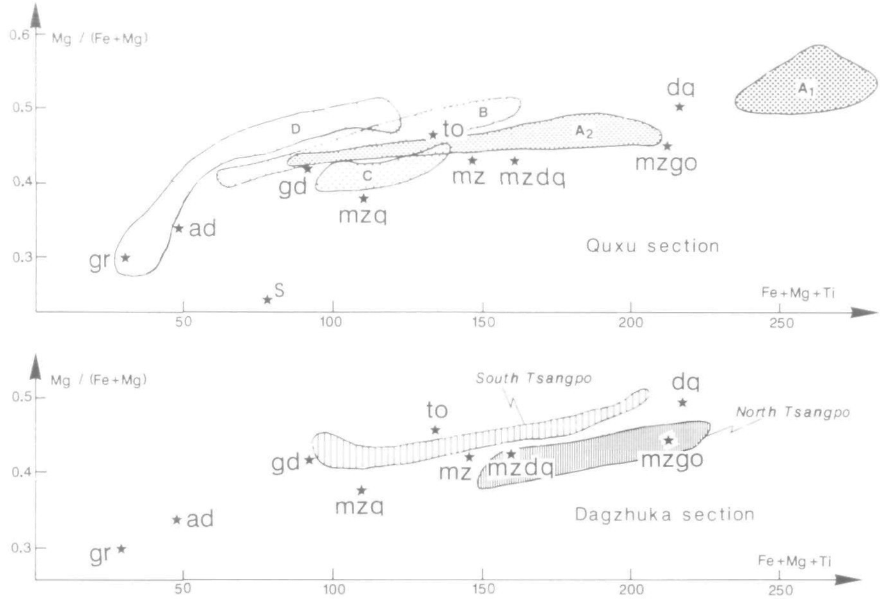

FIG. 11. Mg/(Fe + Mg) *vs.* Fe + Mg + Ti diagrams for the major plutonic units of the Transhimalayan Quxu (A1, A2, B, C, D) and Dagzhuka (North and South Tsangpo) sections (viz. of the Quxu and Dagzhuka super-units). The Fe + Mg + Ti sum is in gram-atoms × 10^3 in 100 g of rock; it is proportional to the dark mineral content in common plutonic rocks (B parameter of La Roche, 1964). Other explanations as in Fig. 4.

values. Old continental crust or sediments dominated by minerals formed during weathering of continental crust, however, are excluded by the combined isotope results (Sheppard *et al.*, 1983). Comparable oxygen isotope data and conclusions have been presented for the Ladakh intrusion of the Transhimalaya batholith, 1000 km or so to the northwest, by Blattner *et al.* (1983).

All of these features suggest a mixed or hybrid origin. Such a hybrid origin is also compatible with the cafemic or alumino-cafemic character of the plutonic units (Table 2) and with the geodynamic location of the batholith. The proposed basic component, which is more basic than any rock analysed here, could carry a dominantly mantle signature, both chemically and isotopically. The acid component could be dominantly of crustal origin, such as relatively young island-arc volcanic material, immature sediments of dominantly volcanic origin, or subducted oceanic crust, hydrothermally altered by seawater, with associated sediments that contain continental derived Nd among other things. According to the differences observed from the batholith *s.st.* to the plutons of its northern edge, the basic contribution tends to decrease from south to north, i.e. on moving off from the suture zone. Finally, the relatively very homogeneous $\delta^{18}O$ values for the large variety of rock types (Fig. 9) implies that the source region was also similarly homogeneous for these isotopic compositions. In contrast, the presence of very abundant microgranular inclusions, which could represent the basic component more or less modified by chemical exchange with the acid component (Leterrier, 1972; Debon, 1975; Leterrier & Debon, 1978), suggests that the mechanical and chemical homogenization of the two presumed source components was not complete. The conspicuous lack of Sr isotope homogenization, both in Tibet (Wang *et al.*, 1981; Jin & Xu, 1984) and Ladakh (Honegger *et al.*, 1982; Schärer *et al.*, 1984*a*), supports this conclusion.

TABLE 3

Mean chemical compositions of the different plutonic types

Belt		*Plutonic unit*	*Rock type*[1]	*n*	SiO_2	Al_2O_3	Fe_2O_3*	MnO	MgO	CaO	Na_2O	K_2O	TiO_2	P_2O_5	L.I.	*Total*	Ba	Rb	Sr
TRANSHIMALAYA	PLUTONS OF THE NORTHERN EDGE	Madian	mzdq/IV	5	58·75	15·51	7·45	0·11	3·25	5·81	3·17	3·22	0·99	0·15	0·80	99·21	483	134	374
		„	(lc)/ad, gr/II, III	3	73·70	13·31	2·16	0·06	0·23	0·86	3·64	4·82	0·22	0·13	0·83	99·96	441	225	108
		Yangbajain	gd/III	1	67·10	15·89	3·21	0·12	0·93	2·63	4·14	3·74	0·39	0·11	0·69	98·95	902	179	351
		„	ad/III	7	70·59	14·69	2·47	0·08	0·64	1·96	3·55	4·46	0·16	0·11	0·56	99·47	690	191	271
		„	lc/gr/I, II	3	75·31	13·14	0·99	0·05	0·09	0·66	3·35	5·07	0·20	0·00	0·45	99·31	385	213	125
		Gu Rong																	
		outer zone	mzdq, (gd)/IV	8	59·53	16·18	7·17	0·11	3·05	5·77	3·43	2·87	0·89	0·25	0·55	99·80	480	120	345
		inter zone	ad, (gr)/IV	8	69·80	14·22	3·10	0·06	0·99	2·46	3·40	4·61	0·47	0·13	0·55	99·79	536	192	239
		inner zone	ad/IV	8	67·74	14·77	4·25	0·08	1·30	3·23	3·20	4·22	0·53	0·14	0·54	100·00	506	178	244
		Lhasa:																	
		North zone	mzdq/IV	2	60·30	16·45	6·76	0·12	2·99	5·85	3·54	2·37	0·84	0·29	0·94	100·45	375	64	375
		South zone	gd, (ad)/III, IV	13	71·86	14·32	2·40	0·07	0·65	2·17	3·79	3·58	0·32	0·10	0·57	99·83	493	102	202
	QUXU SECTION	A1	go/IV	9	50·65	18·76	9·70	0·17	5·27	9·20	3·57	0·48	0·87	0·31	0·50	99·48	180	6–11	749
		A2	dq/IV	6	57·79	17·32	7·21	0·13	3·19	6·54	3·77	1·87	0·76	0·25	0·77	99·60	401	44	528
		„	mzdq/IV	2	59·75	17·70	6·44	0·12	2·87	5·92	3·64	2·40	0·66	0·21	0·61	100·32	448	52	461
		„	gd/III, IV	6	64·33	16·27	4·96	0·09	2·02	4·49	3·84	2·72	0·55	0·20	0·70	100·17	567	76	490
		B	mzdq/IV	4	60·75	16·86	5·48	0·11	2·58	5·44	4·04	2·97	0·63	0·31	0·62	99·79	626	79	724
		„	gd/IV	3	66·05	15·36	4·04	0·08	1·57	3·73	3·81	3·52	0·46	0·15	0·68	99·45	544	102	445
		„	ad/III, IV	2	69·44	14·70	2·80	0·06	0·97	2·64	3·37	4·09	0·21	0·15	0·67	99·10	630	82	409
		C	mzdq/IV	2	60·69	17·13	5·28	0·10	1·97	4·57	4·20	3·14	0·84	0·32	1·00	99·24	889	97	666
		„	mzq/IV	1	62·42	16·62	5·10	0·10	1·88	4·05	3·72	4·20	0·62	0·21	0·86	99·78	931	102	484
		„	gd/IV	4	65·36	15·57	4·45	0·09	1·55	3·76	3·84	3·42	0·65	0·24	0·80	99·73	683	101	466
		D	mzq/IV	2	62·32	15·32	4·59	0·09	2·17	3·62	3·60	4·89	0·55	1·12	0·96	99·23	911	321	532
		„	(lc)/ad/III, IV	8	69·60	14·82	2·35	0·05	0·77	1·97	3·91	4·58	0·34	0·15	0·71	99·25	601	258	392
	DAGZHUKA	North Tsangpo	go/IV	3	53·50	17·76	8·97	0·17	3·80	7·78	3·89	1·63	0·94	0·42	0·50	99·36	334	49	691
			mzdq, mz/IV	3	58·28	16·94	6·91	0·14	2·47	5·32	4·13	3·43	0·84	0·33	0·63	99·42	618	87	521
		South Tsangpo	mzdq/IV	5	60·91	16·04	6·46	0·10	2·77	5·39	3·56	3·18	0·87	0·28	0·47	100·03	494	88	494
			ad/IV	2	66·31	14·68	4·12	0·07	1·56	3·12	3·46	4·40	0·59	0·16	0·78	99·25	542	161	346

NORTH HIMALAYA	PALAEOZOIC	Kangmar	(lc)/ad/II, III	5	73·24	13·59	1·96	0·05	0·49	1·56	3·25	4·31	0·26	0·02	0·51	99·24	460	200	88
		,,	lc/gr/I, II	8	76·02	12·85	1·18	0·04	0·13	0·77	3·18	4·76	0·12	0·00	0·60	99·65	368	271	39–41
		Gyaco La	(lc)/gr/(I), II	9	76·32	12·08	2·01	0·04	0·21	0·59	2·47	5·04	0·28	0·07	0·43	99·54	590	311	35
	CENOZOIC	Gyaco La	(lc)/ad/I	12	72·76	15·32	1·44	0·04	0·39	0·98	3·63	3·95	0·22	0·09	0·79	99·61	396	> 226	142
		,,	ad/II, III	4	72·25	14·50	2·58	0·05	0·88	1·45	3·68	3·91	0·38	0·09	0·60	100·37	495	210	129
		Kari La	(lc)/gd/(I), II	4	71·47	15·47	1·65	0·05	0·77	1·84	3·84	3·56	0·24	0·05	0·61	99·52	569	122	274
HIGH HIMALAYA		Lhozhag	lc/gd/I	1	73·89	15·36	0·64	0·03	0·00	0·83	4·60	3·83	0·00	0·03	0·38	99·59	83	307	55
		,,	lc/ad/I	6	73·66	15·18	0·75	0·03	0·02	0·70	4·05	4·36	0·03	0·04	0·63	99·45	140	308	65
		,,	lc/gr/I	1	73·51	15·61	0·78	0·03	0·07	0·81	3·60	4·93	0·00	0·11	0·65	100·10	179	355	85
		Manaslu. core	lc/ad, (gr)/I	190	73·69	14·85	0·84	0·03	0·11	0·47	4·05	4·55	0·09	0·13	0·84	99·65	205	367	75
		arm	lc/ad, (gr)/I	23	73·94	14·76	0·81	0·02	0·13	0·46	4·14	4·48	0·07	0·13	0·72	99·66	128	—	41
'LESSER HIMALAYA'		Simchar, Ipa, Narayan Than, Eastern Sindhuli Garhi	mesocratic type, (ad), gr/II, III	55	71·33	13·10	3·76	0·06	1·35	1·17	2·59	4·23	0·55	0·18	0·97	99·29	400	249	60
			leuco- and sub-leucocratic type (lc)/gr/I, II	27	74·30	13·46	1·64	0·05	0·35	0·36	2·98	4·95	0·12	0·19	0·88	99·35	176	391	36
		Palung	main type (lc)/(ad), gr/I, II	27	74·51	13·49	1·44	0·05	0·31	0·43	3·24	4·68	0·16	0·25	0·71	99·27	135	429	31

Data from this study; Le Fort (1981); Debon *et al.* (1982); Le Fort *et al* (1983).

[1] Rock type refers to the classification of Debon & Le Fort (1982); lc leucocratic; ad adamellite; dq quartz diorite; gd granodiorite; go gabbro; gr granite, mz monzonite, mzdq quartz monzodiorite; mzq quartz monzonite (Fig. 4); the roman numerals (I to IV here) respectively correspond to rocks with: I muscovite > biotite (by volume), II biotite > muscovite, III biotite, IV biotite + amphibole ± pyroxenes (Fig. 5).

n number of analysed samples

* Total Fe as Fe_2O_3

TABLE 4

REE compositions of selected samples

Belt		*Plutonic unit*	*Sample number*	*Rock type*	La	Ce	Nd	Sm	Eu	Gd	Dy	Er	Yb	Lu	Y	La/Yb
TRANSHIMALAYA	NORTHERN EDGE	Yangbajain	XR 40	ad/III	38·09	72·29	29·00	5·19	1·01	4·33	3·66	2·24	2·27	0·35	24·08	16·8
		Gu Rong														
		outer zone	XR 150	mzdq/IV	20·50	46·31	22·21	4·53	0·90	4·12	3·95	2·33	2·18	0·32	25·25	9·4
		inter zone	XR 121	ad/IV	44·76	86·04	40·02	7·61	1·63	6·51	5·61	2·97	2·85	0·41	33·98	15·7
		inner zone	XR 129	ad/IV	23·53	46·65	22·43	4·55	0·86	3·93	4·02	2·43	2·49	0·39	26·90	9·4
		Lhasa	XR 79	mzdq/IV	16·86	37·84	19·62	4·09	1 13	4·26	3·90	2·21	2·15	0·30	24·18	7·8
		„	XR 89	ad/III	25·39	49·44	20·32	3·75	0·77	3·38	3·51	2·00	2·21	0·32	21·63	11·5
	QUXU SECTION	A_1	XR 463	go/IV	9·45	25·28	15·04	3·06	1·06	3·11	2·61	1·50	1·25	0·19	15 59	7 6
		A_2	XR 575	dq/IV	14·80	28·04	14·96	2·88	0·93	2·82	2·45	1·50	1·30	0·20	15·14	11·4
		„	XR 529	gd/IV	15·35	32·94	16·85	3·22	0·75	2·99	2·77	1·84	1·73	0·24	19·08	8·9
		B	XR 502	mzdq/IV	34·88	65·34	25·32	4·30	1·05	2·95	1·87	1·12	0·93	0·13	11·00	37·5
		„	XR 453	gd/IV	16·50	34·87	16·58	3·18	0·72	2·61	2·35	1·51	1·46	0·21	15·91	11·3
		C	XR 537	mzdq/IV	38·40	88·26	40·06	6·97	1 52	5·65	4·13	2·38	2·15	0·30	25·63	17·9
		„	XR 543	mzq/IV	31·32	73·97	34 59	6·46	1·26	5 23	4·52	2·65	2·59	0·34	28·58	12·1
		D	XR 525	mzq/IV	79·52	150·62	57·88	9·03	1·48	6·00	3 42	1·81	1·47	0·20	18·44	54·1
		„	XR 514	ad/III	47·73	90·08	32·27	4·55	0·92	2·96	1·48	0·83	0·59	0·07	8·19	80·9
DAGZHUKA		North Tsangpo	XR 383	go/IV	19·64	48·95	25·54	5·36	1·62	4·87	4·08	2·28	2·05	0·28	24·84	9·6
		South Tsangpo	XR 370	ad/IV	18·09	38·64	18·93	3 74	0·79	3 11	2·63	1·53	1·41	0·21	16·35	12·8

NORTH HIMALAYA	PALAEOZOIC	Kangmar	XR 253	ad/III	28·81	58·75	23·31	4·92	0·89	4·65	4·48	2·90	2·90	0·45	30·63	9·9
		”	XR 250	lc/ad/II	33·33	63·45	25·45	5·23	0·73	4·96	4·95	3·01	3·20	0·47	34·21	10·4
		”	XR 238	lc/gr/II	12·23	24·18	9·62	1·79	0·29	1·52	1·49	1·01	1·16	0·18	10·52	10·5
		”	XR 261	lc/gr/I	15·03	34·34	16·83	4·36	0·47	4·49	5·83	3·93	4·42	0·65	43·60	3·4
		Gyaco La	XR 314	lc/gr/II	38·49	79·43	34·04	7·22	0·76	7·00	7·68	4·68	4·53	0·63	51·39	8·5
		”	XR 343	lc/gr/II	32·69	69·10	29·64	6·82	0·58	6·82	8·21	4·98	4·92	0·71	54·76	6·6
		”	XR 326	lc/gr/I	33·82	73·36	28·76	7·03	0·60	6·38	7·89	4·95	4·83	0·70	55·02	7·0
	CENOZOIC	Gyaco La	XR 328	ad/III	29·14	60·08	24·14	5·27	0·89	4·59	5·42	3·45	3·40	0·51	38·36	8·6
		”	XR 316	ad/II	18·68	36·82	17·06	3·68	0·65	3·67	5·22	3·50	3·87	0·55	39·04	4·8
		”	XR 322	lc/ad/I	11·54	25·13	10·48	2·68	0·64	2·49	2·53	1 59	1·59	0·24	18·89	7·3
		”	XR 323	ad/I	23·76	50·33	22·24	4·28	1·06	3·51	2·26	1·06	0·80	0·11	11·55	29·7
		Kari La	XR 223	gd/II	18·98	39·51	18·04	3·60	0·87	2·68	1·72	0·96	0·77	0·13	10·30	24·6
		”	XR 225	lc/gd/I	11·58	25·86	10·98	2·52	0·63	2·16	1·58	0·96	0·76	0·12	9·94	15·2
HIGH HIMALAYA		Lhozhag	XR 189	lc/gd/I	5·29	11 64	5·05	1·55	0·40	1·64	1·30	0·61	0·45	0·07	7·79	11·8
		”	XR 183	lc/ad/I	7·91	17·69	8·10	2·24	0·51	2·32	1·14	0·50	0·23	0·03	5·21	34·4
		”	XR 191	lc/ad/I	12·35	29·10	12·38	3·55	0·54	3·30	1·57	0·50	0·32	0·03	7·34	38·6
		”	XR 191[1]	muscov.	—	37·4	20·40	4·57	0·15	3·14	0·94	0·22	0·18	—	—	—
		Manaslu	DK 201	lc/ad/I	0·27	1·79	0·40	0·26	0·02	0·36	0·81	0·25	0·39	0·05	4·12	0·7
			DK 46	lc/gd/I	1·02	0·96	0·74	0·52	0·01	0·65	1·15	0·43	0·53	0·07	6·43	1·9
			DK 170	lc/ad/I	8·19	12·28	4·74	1·46	0·28	1·58	1·92	0·70	0·64	0·10	11·44	12·8
			DK 195	lc/gr/I	13·71	28·14	12·62	3·67	0·78	3·94	4·82	1·70	1·25	0·16	24·77	11·0
			average	lc/ad/I												
'LESSER HIMALAYA'		Simchar	KP 25	gr/III	33·00	67·55	29·78	6·67	1·07	6·26	6·14	3·05	3·43	0·49	40·17	9·6
		”	KP 170	gr/II	33·99	73·49	30·96	7·09	1·10	6·31	6·12	3·11	3·42	0·47	41·18	9 9
		”	KP 428	gr/II	16·11	38·67	14·58	3·74	0·50	3·16	4·60	2·87	3·47	0·51	33·74	4·6
		”	SR 91	lc/gr/II	18·35	38·31	17·91	4·29	0·61	4·07	5·23	2·80	3·12	0·41	36·77	5·9
		Ipa	KP 243	gr/II	30·10	60·94	28·04	6·18	1·10	5·54	5·80	3·04	3·36	0·48	38·93	9·0
		”	KP 246	lc/gr/I	12·29	25·56	11·02	2·93	0·42	2·48	3·26	1·58	1·89	0·26	21·08	6·5
		Palung	KP 136	ad/II	18·88	40·38	18·66	4·59	0·50	4·03	4·48	2·20	2·58	0·37	29·63	7·3
		”	KP 217	lc/gr/I	8·11	15·40	7·32	1·98	0·26	1·92	2·60	1·38	1·65	0·26	19·27	4·9
		”	KP 316	lc/gr/I	2·95	6·27	2·69	0·88	0·11	0·82	1·11	0·62	0·84	0·14	8·18	3·5

Values in p.p.m.

[1] Muscovite XR 191 analysed by isotope dilution (C. Alibert).

The bulk chemistry of most of these samples is given in Table 5. Other explanations as in Table 3.

TABLE 5

Chemical and oxygen compositions of selected samples

Belt	*Plutonic unit*	*Sample number*	*Rock type*	SiO_2	Al_2O_3	Fe_2O_3t	MnO	MgO	CaO	Na_2O	K_2O	TiO_2	P_2O_5	L.I.	*Total*	Ba	Rb	Sr	$\delta^{18}O$ ‰
TRANSHIMALAYA, NORTHERN EDGE	Yangbajain	XR 40	ad/II	69·37	15·22	2·99	0·09	0·84	2·32	3 55	4·36	0·42	0·16	0·57	99·89	745	167	303	7·6
	"	XR 53	lc/gr/II	75·34	12·99	1·06	0·06	0·13	0·66	3·36	5·07	0·20	0·00	0·44	99·31	284	213	114	8·5
	Gu Rong.																		
	outer zone	XR 150	mzdq/IV	59·36	16 52	7·17	0·12	3·10	5·87	3·49	2 99	0·84	0·22	0·31	99·99	380	128	312	7·4
	inter zone	XR 121	ad/IV	66·88	15 37	3·90	0·06	1·05	3·02	3 70	4·31	0·60	0·27	0·73	99 89	813	158	392	7 5
	inner zone	XR 129	ad/IV	69·23	14·75	3 87	0·06	0·99	2·81	3·18	4·44	0·46	0·19	0·48	100·46	501	192	209	7 6
	Lhasa	XR 89	ad/III	71 20	14·71	2·56	0·08	0·47	2 13	3 59	3 76	0·31	0·17	0·40	99·38	484	101	215	7·9
TRANSHIMALAYA, QUXU SECTION	A_1	XR 465	go/IV	50·04	19·00	9·93	0·17	5·31	8 98	3·57	0·33	0·92	0·38	0·09	98·72	175	< 10	778	—
	"	XR 463	go/IV	52·03	18·12	9 64	0·16	5 22	8·93	3 80	0·82	0·85	0·31	0·57	100·45	227	13	730	6 8
	A_2	XR 457	dq/IV	58·36	17·10	7·27	0·12	3·46	6·48	3 78	1 95	0·73	0·26	0·95	100·46	390	36	569	—
	"	XR 575	dq/IV	57·05	17·32	7·09	0·14	3·16	6·60	3·78	1 74	0·72	0·18	1·00	98·78	471	33	512	7 5
	"	XR 529	gd/IV	64 43	15 69	5·05	0·09	2 10	4·52	3·48	3·12	0·49	0·15	0·52	99·64	531	102	348	—
	B	XR 502	mzdq/IV	62·45	16·08	4·57	0·09	2 13	4·44	4·04	3·39	0·49	0·30	0·74	98 72	893	69	699	—
	"	XR 453	gd/IV	64·24	15 44	4·63	0·09	1·83	3·99	3·92	3·26	0·48	0·20	0·71	98·79	473	85	469	8·1
	"	XR 545	ad/IV	69·78	14·74	2·81	0·05	0·95	2·79	3·08	4 39	0·33	0·15	0·55	99·62	825	99	440	8·0
	C	XR 537	mzdq/IV	61·11	16·49	5·56	0·11	2·26	4 69	4·03	3·18	0·85	0·30	0·69	99 27	827	110	629	7 7
	"	XR 543	mzq/IV	62·42	16·62	5·10	0·10	1 88	4·05	3 72	4·20	0·62	0·21	0·86	99·78	931	102	484	—
	D	XR 525	mzq/IV	61 91	15·25	4·87	0·08	2·12	3·45	3·63	4·66	0·57	1 87	1·06	99 47	890	239	514	—
	"	XR 514	ad/III	67·66	15 33	2·83	0·06	1·24	2 19	3·92	4·40	0·44	0·26	0·81	99 14	581	216	455	9 2
TRANSHIMALAYA, DAGZHUKA	North Tsangpo	XR 383	go/IV	53·27	17·75	9·16	0·18	3·61	7 37	4 10	1·79	1·02	0·44	0·34	99·03	387	46	707	6 8
	South Tsangpo	XR 370	ad/IV	65 95	14 75	4 30	0·07	1 53	3 29	3 50	4·36	0·63	0·16	0·62	99 16	548	157	351	7·5

NORTH HIMALAYA	PALAEOZOIC	Kangmar	XR 250	lc/ad/II	72·92	14·24	1·96	0·05	0·43	1·66	3·38	4·39	0·23	—	0·42	99·68	443	224	85	8·9
		"	XR 238	lc/gr/II	76·52	12·78	1·15	0·04	0·09	0·92	3·07	4·54	0·13	—	0·40	99·64	598	244	52	9·7
		"	XR 243	lc/gr/I	77·38	12·78	1·01	0·03	0·03	0·60	3·37	4·72	0·06	—	0·15	100·13	336	268	28	—
		Gyaco La	XR 314	lc/gr/II	75·75	12·71	2·27	0·04	0·22	0·79	2·76	4·74	0·32	0·06	0·40	100·06	608	296	37	10·6
		"	XR 327	lc/gr/II	76·57	11·33	1·92	0·04	0·31	0·54	2·15	4·98	0·23	0·11	0·47	98·65	563	265	38	—
		"	XR 343	lc/gr/II	76·93	12·13	1·64	0·04	0·21	0·45	2·73	5·06	0·23	0·02	0·41	99·85	532	360	25	10·9
	CENOZOIC	Gyaco La	XR 316	ad/II	72·40	14·81	2·34	0·05	0·57	1·16	3·74	4·08	0·31	0·04	0·62	100·12	388	254	96	12·0
		"	XR 323	ad/I	71·60	15·79	1·75	0·03	0·53	0·98	3·41	4·10	0·32	0·13	0·88	99·52	527	219	167	13·3
		"	XR 319	lc/ad/I	72·76	15·51	1·50	0·04	0·35	0·95	3·50	4·09	0·24	0·15	0·79	99·88	428	248	140	—
HIMALAYA		Lhozhag	XR 191	lc/ad/I	73·07	15·47	0·90	0·03	0·00	0·68	3·85	4·20	0·07	0·11	0·65	99·03	130	387	60	14·0
		"	XR 183	lc/ad/I	73·72	15·03	0·69	0·02	0·03	0·56	4·08	4·27	0·04	0·01	0·69	99·14	117	284	56	13·0
		"	XR 188	lc/ad/I	73·99	15·14	0·74	0·03	0·03	0·69	3·89	4·63	0·00	0·00	0·73	99·87	162	211	59	11·5
		Manaslu[1] (core)	Average	lc/ad, (gr)/I	73·69	14·85	0·84	0·03	0·11	0·47	4·05	4·55	0·09	0·13	0·84	99·65	205	367	75	12·2
'LESSER HIMALAYA'		Simchar	KP 25	gr/III	70·83	13·06	3·93	0·05	1·56	1·37	2·60	4·09	0·58	0·11	1·00	99·18	399	214	67	11·4
		"	KP 170	gr/II	71·03	13·51	3·59	0·05	1·29	1·09	2·59	4·49	0·55	0·14	0·90	99·24	424	283	64	—
		"	KP 428	gr/II	73·50	13·60	2·31	0·04	0·71	0·64	2·59	5·23	0·31	0·22	0·79	99·94	266	328	38	—
		"	SR 91	lc/gr/II	73·36	13·47	1·82	0·02	0·46	0·53	2·88	5·29	0·22	0·30	0·84	99·19	230	394	31	12·8
		Ipa	KP 243	gr/II	73·07	12·94	3·29	0·07	1·11	1·15	2·71	4·21	0·48	0·17	0·92	100·12	398	266	67	—
		"	KP 246	lc/gr/I	74·11	13·33	1·69	0·05	0·38	0·50	3·14	4·78	0·18	0·19	0·86	99·21	127	396	28	—
		Palung	KP 136	ad/II	74·63	13·13	2·26	0·07	0·54	0·78	3·05	4·12	0·29	0·23	0·73	99·83	182	336	44	—
		"	KP 217	lc/gr/I	74·32	13·95	1·33	0·06	0·21	0·35	3·52	4·75	0·12	0·21	0·37	99·19	119	371	31	12·3
		"	KP 316	lc/gr/I	76·41	12·99	0·50	0·02	0·03	0·12	3·40	4·89	0·06	0·23	0·52	99·17	35	555	27	—

In each plutonic unit, the samples are arranged according to decreasing dark mineral contents.
[1] Oxygen isotope composition for Manaslu after Vidal *et al* (1984)
Other explanations as in Table 3.

THE THREE HIMALAYA PLUTONIC BELTS (NORTH, HIGH, AND 'LESSER' HIMALAYA)

Geological setting

South of both the Transhimalaya belt and of the Indus–Tsangpo suture zone, three different belts of granitoids occur along the Himalaya. From north to south they are the North Himalaya (or Lhagoi Kangri), the High Himalaya, and the 'Lesser Himalaya' belts (Fig. 1).

The North Himalaya belt is composed of two groups of granitoids as domes within metasedimentary rocks of dominantly Upper Palaeozoic to Mesozoic age (e.g. Academia Sinica, 1980; Wang *et al.*, 1981; Debon *et al.*, 1982, 1983; Burg, 1983; Le Fort, 1985). This study considers two domes of the Palaeozoic more or less gneissic porphyritic granite group (Gyaco La, Kangmar) and two of the Cenozoic two-mica adamellite group (Gyaco La, Kari La) (Fig. 2). The two groups may be associated (Gyaco La) or independent (e.g. Kangmar, Kari La).

The Cenozoic plutons of the High Himalaya belt (Fig. 2) were emplaced into rocks of up to Cretaceous age in the Tibetan sedimentary series (e.g. Le Fort, 1973, 1981). The Lhozhag and Manaslu plutons are considered here.

The discontinuous 'Lesser Himalaya' (Fig. 2) is a belt of Palaeozoic granitoids. They occur only in the overthrust slab of the Main Central Thrust (MCT) (e.g. Le Fort *et al.*, 1980, 1983). Five plutons of the Kathmandu nappe, Simchar, Palung, Ipa, Narayan Than, and Eastern Sindhuli Garhi were studied.

Petrographical and geochemical characteristics

The Himalaya granitoids are fundamentally different from the Transhimalaya ones (e.g. Le Fort, 1973, 1981, 1985; Tu *et al.*, 1981, 1982; Debon *et al.*, 1982; Blattner *et al.*, 1983; Le Fort *et al.*, 1983; Sheppard *et al.*, 1983; Jin & Xu, 1984; Figs. 4–6, 8, 9, 12). Most of them are granites or adamellites (Fig. 4, Table 3), always peraluminous with a variable amount of biotite (with Mg/(Fe+Mg) ratios ranging from 0·10 to 0·45) and muscovite (Fig. 5), and are commonly leucocratic (Fig. 6). Tourmaline, cordierite and, to a lesser extent, garnet, sillimanite, and andalusite may occur in some of them (Table 8). Almost all these granitoids are Rb-rich and Sr-poor (Table 3). They all belong to different types of aluminous magmatic associations (Fig. 5, Table 8).

The Palaeozoic North and 'Lesser' Himalaya granitoids have remarkably similar REE patterns (Fig. 8, Table 4) which compare well with granitoids with analogous chemistry and mineralogy from other regions, in particular with Fourcade's (1981) 'type 3' two-mica plutonic rocks. In each of these belts, the REE abundances systematically decrease from the darkest to the most light-coloured rocks, suggesting that the content in REE is closely related to the amount of accessory minerals. The High Himalaya granitoids have particularly low or very low REE contents (Cocherie, 1977; Vidal *et al.*, 1984; Fig. 8, Table 4). The lowest REE contents correspond to two samples of the Manaslu pluton which are remarkably poor in Th (*c.* 1 p.p.m.). This relationship suggests that monazite may be the main host-mineral for REE (Cuney *et al.*, 1984). Finally, the REE patterns of the Cenozoic North Himalaya granitoids display similarities with those of both the Palaeozoic and High Himalaya ones (Fig. 8, Table 4).

The oxygen isotope compositions of the North, High and 'Lesser' Himalaya (Table 5, Fig. 9) fall into two groups both of which are enriched in ^{18}O relative to the Transhimalaya batholith. The Cenozoic North, High and Palaeozoic 'Lesser' Himalaya all have particularly high $\delta^{18}O$ values (11·4 to 14·0 per mil) and, from an O-isotope point of view, are

TABLE 6

Summary of post 1980 radiometric ages from the literature

Belt		*Plutonic unit or super-unit*	*Comments*
TRANSHIMALAYA	NORTHERN PLUTONS	Yangbajain	By Rb-Sr isochron on 6 whole rocks: *46·7 Ma* ± 3, Sr_i = 0·7070 ± (1) (Debon *et al.*, 1982)/By Rb-Sr on one whole rock-biotite pair *49·0 Ma* (Xu *et al.*, 1985)/By U-Pb on zircons. *c.* 50 Ma (Xu *et al.*, 1985).
TRANSHIMALAYA	NORTHERN PLUTONS	Lhasa-Gu Rong	By Rb-Sr isochron on 7 whole rocks. *55·8 Ma* ± 9·9, Sr_i = 0·7057 (Jin & Xu, 1984)/By Rb-Sr isochron on minerals: *59·4 Ma* ± 0·5, Sr_i = 0·7053 (Jin & Xu, 1984)/By U-Pb on zircons: *c. 53 Ma* (Schärer *et al.*, 1984*b*).
TRANSHIMALAYA	QUXU SECTION	A1 – A2	By K-Ar isochron on 3 whole rocks and 4 minerals: *49·4 Ma* ± 0·7 (Debon *et al.*, 1985).
TRANSHIMALAYA	QUXU SECTION	B	By U-Pb on zircons: *41·1 Ma* ± 0·4, *41·7 Ma* ± 0·4 (Schärer *et al.*, 1984*b*).
TRANSHIMALAYA	QUXU SECTION	D	By Rb-Sr 'errorchron' on 5 whole rocks. *44·3 Ma* ± 14, Sr_i = 0·7067 ± (4) (Debon *et al.*, 1982).
TRANSHIMALAYA	QUXU SECTION	? near Quxu	By Rb-Sr isochron on 6 whole rocks: *52·4 Ma* ± 11·8, Sr_i = 0·7052 ± (6) (Jin & Xu, 1984).
TRANSHIMALAYA	DAGZHUKA	North Tsangpo	By ^{39}Ar-^{40}Ar on minerals between *93* and *113 Ma* (Maluski *et al.*, 1982)/By Rb-Sr on one whole rock-biotite pair *87·9 Ma* (Debon *et al.*, 1983)/By U-Pb on zircons from diorites: *93·4 Ma* ± 1·0, *94·2 Ma* ± 1·0 (Schärer *et al.*, 1984*b*).
TRANSHIMALAYA	DAGZHUKA	South Tsangpo	By Rb-Sr on one whole rock-biotite pair *92·9 Ma* (Debon *et al.*, 1983).
NORTH HIMALAYA	PALAEOZOIC	Kangmar	By Rb-Sr isochron on 6 whole rocks: *485 Ma* ± 6, Sr_i = 0·7186 ± (18) (Wang *et al.*, 1981)/By Rb-Sr isochron on 5 whole rocks *484 Ma* ± 14, Sr_i = 0·7140 ± (12) (Debon *et al.*, 1982)/By Rb-Sr isochron on 8 whole rocks: *434·7 Ma* ± 37·3, Sr_i = 0·7207 ± (9) (Jin & Xu, 1948)/By K-Ar on one biotite: *31·8 Ma* (Zhang *et al.*, 1981)/By K-Ar isochron on 5 biotites *14·6 Ma* ± 0·5 (Debon *et al.*, 1985)/By ^{39}Ar-^{40}Ar on 2 micas: *17·3* and *21·7 Ma* (Maluski, 1984).
NORTH HIMALAYA	PALAEOZOIC	Gyaco La	By K-Ar on one biotite: *12·8 Ma* ± 1·3 (Debon *et al.*, 1985).
NORTH HIMALAYA	CENOZ.	Gyaco La	By K-Ar isochron on 2 biotites and 2 muscovites: *13·3 Ma* ± 0·4 (Debon *et al.*, 1985).
NORTH HIMALAYA	CENOZ.	Kari La	By K-Ar isochron on 3 whole rocks and 3 biotites. 10·8 Ma ± 0·8 (Debon *et al.*, 1985)
HIGH HIMALAYA		Lhozhag	By Rb-Sr on 2 whole rock-muscovite pairs: *15·1 and 15·8 Ma*, Sr_i = 0·7285 and 0·7269 (Debon *et al.*, 1983)/By K-Ar on 2 muscovites. *13·3 Ma* ± 1·0 (Debon *et al.*, 1985)
HIGH HIMALAYA		Manaslu	By Rb-Sr on 6 whole rock-muscovite pairs: *15·3 to 20·5 Ma* (Vidal *et al.*, 1982)/By Rb-Sr isochron on 11 whole rocks: *18·1 Ma* ± 0·5, Sr_i = 0·7470 ± (10) (Deniel *et al.*, 1983*a*, *b*)
'LESSER HIMALAYA'		Simchar	By Rb-Sr isochron on 7 whole rocks: *466 Ma* ± 40, Sr_i = 0·7205 ± (46) (5 samples) and *511 Ma* ± 55, Sr_i = 0·7085 ± (48) (7 samples) (Le Fort *et al.*, 1983).
'LESSER HIMALAYA'		Ipa	By Rb-Sr on one whole rock-biotite pair *14 Ma* (Le Fort *et al.*, 1983).
'LESSER HIMALAYA'		Palung	By whole rock Rb-Sr isochron. *486 Ma* ± 10, Sr_i = 0·720 (Beckinsale, in Mitchell, 1981)/By U-Pb on zircons and monazites *470 Ma* ± 4 (Schärer & Allègre, 1983).

indistinguishable. Oxygen isotope data on other High Himalaya granites and potential metasedimentary source rocks are equally ^{18}O-rich (Blattner *et al.*, 1983; Vidal *et al.*, 1984). The Palaeozoic North Himalaya defines a distinct group with $\delta^{18}O$ = 8·9 to 10·9. For all these Himalaya granitoids, there is a good positive correlation between $\delta^{18}O$ and the aluminous index (A; Fig. 9), the mica content or the muscovite/biotite ratio. There is no general correlation with SiO_2 content.

Although the Himalaya granitoids are similar in many respects there are also specific differences (Table 8). Compared with the Cenozoic plutons, the Palaeozoic ones are porphyritic, often with gneissic textures, sometimes contain dark igneous microgranular inclusions (up to some 5 per cent by volume) and are dominantly granitic in composition (Fig. 4, Table 3). The Palaeozoic plutons are typically quartz-rich but poor in feldspars (Fig. 6) and alkalis (mainly in Na). Among the Palaeozoic granitoids themselves, those of the 'Lesser Himalaya' are usually richer in dark minerals, more aluminous (Fig. 5) and higher in $\delta^{18}O$ than the North Himalaya, with their quartz content remaining conspicuously constant

TABLE 7

Rb–Sr isotope data (this study)

Belt	Plutonic unit	Sample number	Sam. mat.[1]	Rock type[2]	Anal. mat.[3]	Rb p.p.m.	Sr p.p.m.	$^{87}Rb/^{86}Sr$	$^{87}Sr/^{86}Sr$	Ages Ma	Initial Sr
TRANSHIMALAYA — PLUTONS OF THE NORTHERN EDGE	Yangbajain	XR 40	+	ad/III	WR	162	331	1·42 ± 0·06	0·7080 ± (3)	49·2	0·7071
	,,	,,	+	,,	Bi	839	13	183·44 ± 4·91	0·8352 ± (1)		
	Gu Rong outer zone	XR 150	+	mzdq/IV	WR	139	334	1·21 ± 0·03	0·7061 ± (2)	48·9	0·7052
		,,	+	,,	Bi	738	11	197·78 ± 11·04	0·8426 ± (6)		
	Gu Rong inter zone	XR 121	+	ad/IV	WR	149	406	1·06 ± 0·03	0·7066 ± (7)	55·6	0·7058
		,,	+	,,	Bi	847	6	392·35 ± 57·84	1·0158 ± (73)		
	Gu Rong inner zone	XR 129	+	,,	WR	183	230	2·30 ± 0·06	0·7060 ± (1)	51·8	0·7043
		,,	+	,,	Bi	791	7	333·72 ± 6·71	0·9499 ± (5)		
	Lhasa	XR 89	+	ad/III	WR	105	234	1·30 ± 0·01	0·7064 ± (2)	59·7	0·7053
	,,	,,	+	,,	Bi	485	9	159·27 ± 2·99	0·8404 ± (7)		
	,,	XR 106	+	gd/III	WR	108	187	1·67 ± 0·04	0·7076 ± (2)	51·2	0·7063
	,,	,,	+	,,	Bi	730	8	251·46 ± 3·45	0·8892 ± (8)		
TRANSHIMALAYA — QUXU SECTION	A1	XR 463	+	go/IV	WR	11	779	0·041 ± 0·001	0·7045 ± (4)		
	,,	XR 465	+	,,	WR	2	825	0·007 ± 0·003	0·7050 ± (1)		
	A2	XR 457	+	dq/IV	WR	40	611	0·19 ± 0·01	0·7049 ± (1)	50·4	0·7048
	,,	,,	+	,,	Bi	321	11	87·97 ± 9·24	0·7678 ± (2)		
	,,	XR 575		,,	WR	48	548	0·25 ± 0·01	0·7051 ± (2)	40·4	0·7049
	,,	,,		,,	Bi	390	9	128·39 ± 7·51	0·7786 ± (6)		
	B	XR 453	+	gd/IV	WR	84	484	0·50 ± 0·01	0·7051 ± (1)	44·1	0·7048
	,,	,,	+	,,	Bi	572	13	127·00 ± 3·18	0·7845 ± (2)		
	C	XR 537		mzdq/IV	WR	118	661	0·51 ± 0·01	0·7045 ± (2)	48·7	0·7042
	,,	,,	·	,,	Bi	651	13	146·27 ± 2·93	0·8054 ± (1)		
TRANSHIMALAYA — DAGZHUKA	North Tsangpo	XR 383	+	go/IV	WR	45	773	0·17 ± 0·01	0·7047 ± (6)	87·9	0·7045
		,,	+	,,	Bi	300	19	45·11 ± 0·52	0·7609 ± (1)		
	South Tsangpo	XR 370	+	ad/IV	WR	140	377	1·07 ± 0·01	0·7050 ± (1)	92·9	0·7036
		,,	+	,,	Bi	706	13	161·72 ± 19·64	0·9171 ± (10)		

NORTH HIMALAYA	PALAEOZOIC	Kangmar	XR 238	+	lc/gr/II	WR	250	65	11·12±0·19	0·7901± (1)	7·1	0·7889
			„	+	„	Bi	1471	10	447·90±28·59	0·8342±(27)		
		Gyaco La	XR 314	·	lc/gr/II	WR	304	38	23·32±0·34	0·8691± (2)	6·5	0·8669
		„	„	·	„	Bi	1604	4	1162·40±79·39	0·9744±(23)		
		„	XR 327	·	„	WR	258	38	19·65±0·24	0·8610±(15)	—	
		„	XR 343	·	„	WR	351	29	34·68±0·46	0·9331± (6)	—	
		„	XR 353	·	gr/II	WR	362	37	28·57±0·91	0·8899± (2)	—	
	CENOZOIC	Gyaco La	TC 74	·	lc/ad/I	WR	223	91	7·07±0·17	0·7477± (1)	—	
		„	TC 75	·	„	WR	229	166	3·98±0·08	0·7420± (1)	—	
		„	XR 316		ad/II	WR	242	117	6·01±0·17	0·7438± (1)	7·1 ±1·2	0·7432 ±0·0004
		„	„	·	„	Bi	1294	9	416·48±7·74	0·7835± (8)		
		„	„	·	„	Mu	627	16	117·11±1·13	0·7570± (6)		
		„	XR 319	·	lc/ad/I	WR	239	173	4·02±0·12	0·7410± (1)	—	
		„	XR 323	·	ad/I	WR	211	204	2·99±0·13	0·7422± (1)	8·4 ±5·4	0·7418 ±0·00025
		„	„		„	Bi	1124	9	356·28±6·14	0·7912±(37)		
		„	„	·	„	Mu	430	64	19·59±0·78	0·7430± (3)		
		„	XR 344	+	lc/gd/I	WR	306	24	37·02±0·96	0·7685± (2)	—	
		„	XR 348	+	lc/gr/I	WR	232	57	11·80±0·19	0·7370± (3)	—	—
		„	XR 363	·	ad/I	WR	180	214	2·43±0·03	0·7456± (1)		
HIGH HIMALAYA		Lhozhag	XR 182	+	lc/ad/I	WR	398	92	12·48±0·23	0·7272± (1)	—	
		„	XR 183	+	„	WR	405	69	17·10±0·18	0·7308± (4)	15·8	0·7269
		„	„	+	„	Mu	1007	10	288·81±6·72	0·7918± (8)		
		„	XR 188	+	„	WR	402	69	16·82±0·70	0·7365± (1)	—	—
		„	XR 189	+	lc/gd/I	WR	320	64	14·50±0·47	0·7334± (3)	—	
		„	XR 191	+	lc/ad/I	WR	431	69	17·99±0·34	0·7323± (1)	15·1	0·7285
		„	„	+	„	Mu	1447	8	516·61±6·74	0·8389± (4)		

[1] Sam. mat., sampled material (cross, outcrop; point, boulder).
[2] Rock type defined as in Table 3.
[3] Anal. mat., analysed material (WR whole rock, Bi biotite, Mu muscovite).

TABLE 8

Petrographic and chemical discrimination criteria between the Himalaya granitoids

Belt	Age	Plutonic unit	Main rock type	K/(Na+K)[1]	Mu > Bi (I)	Bi > Mu (II)	Bi (III)	Quartz content[1] %	Feldspar (+Mu) content[1] %	An % in plagioclase[2]	Dark mineral content %[1]	Mg/(Fe+Mg)[1]	$\delta^{18}O$ ‰[1]	$^{87}Sr/^{86}Sr$ initial	Miscellaneous	Microgranular inclusions	Type of ALUMINOUS association[3]
NORTH HIMALAYA	PALAEOZOIC	Kangmar	granite/ (adamellite)	0·485 var	(X)	X	(X)	36·4 high	58·6 low	23–16	5·0 var	0·23 low var.	9·3 high	~0·71[illegible] high	(porphyritic)/ very gneissified	very rare	quartz rich/subleuco- to leucocratic/ sodi-potassic to potassic/low aluminous
NORTH HIMALAYA	PALAEOZOIC	Gyaco La	granite	0·57	(X)	X		41·4 very high	52·5 low	37–17	6·1	0·17 low var	10·8 high	—	porphyritic/ gneissified	rare	quartz rich/subleuco- to leucocratic/ potassic/moderately aluminous
NORTH HIMALAYA	CENOZOIC	Gyaco La	adamellite	0·42	X	(X)	(X)	34·0 high	59·1 var	26–13	6·9 var	0·37 high var	12·7 very high	~0·74[illegible] very high	(andalusite, sillimanite)	?	quartz rich (to quartz normal)/mesocratic to leucocratic/sodic/highly aluminous (var.)
NORTH HIMALAYA	CENOZOIC	Kari La	granodiorite	0·38	(X)	X		31·5	60·8		7·7 var	0·475 high var		-		very rare	quartz normal/subleuco- to leucocratic/ sodic/moderately aluminous
HIGH HIMALAYA	CENOZOIC	Lhozhag	adamellite	0·41 var	X			31·8	66·4 high	14–8	1·8 very low	0·06 very low	12·8 very high	~0·7[illegible]8 very high	very frequent tourmaline	no	quartz poor/very leucocratic/mainly sodic/ highly aluminous (var.)
HIGH HIMALAYA	CENOZOIC	Manaslu	adamellite	0·42 var	X			31·9	65·4 high	19–1	2·7 very low	0·22 low	12·2 very high	0·750 very high	very frequent tourmaline (sillimanite)	no	quartz poor/very leucocratic/mainly sodic/ highly aluminous (var.)
'LESSER HIMALAYA'	PALAEOZOIC	Simchar, Ipa, Narayan Than, dark facies	granite	0·52		X	X	37·5 high	46·6 very low, var	—	15·9 high var	0·42 high	11·4 very high	0·7085	porphyritic/ (gneissified)/ cordierite	very frequent	bimodal association/quartz rich/mesocratic to leucocratic/sodi-potassic to potassic/highly aluminous
'LESSER HIMALAYA'	PALAEOZOIC	Simchar, Ipa, Narayan Than, light-c facies	granite	0·52	X	X		37·5 high	56·7 low var	—	5·8	0·30	12·8 very high	0·7205 high	(gneissified)/ tourmaline/ cordierite	rare	
'LESSER HIMALAYA'	PALAEOZOIC	Palung main facies	granite	0·49	X	X		36·8 high	58·2 low var	—	5·0 var	0·31 var	12·3 very high	0·720 high	(porphyritic)/ (gneissified)/ tourmaline	rare	quartz rich (to quartz normal)/(mesocratic) to leucocratic/sodi-potassic to potassic/ highly aluminous

Mu muscovite, Bi biotite, var variable, light-c light-coloured.

[1] Most of these values are averages calculated from data in Tables 3, 5, 6, 7

[2] Anorthite content in plagioclase (An %) corresponds to extreme values

[3] The typology refers to the classification of Debon & Le Fort (1982)

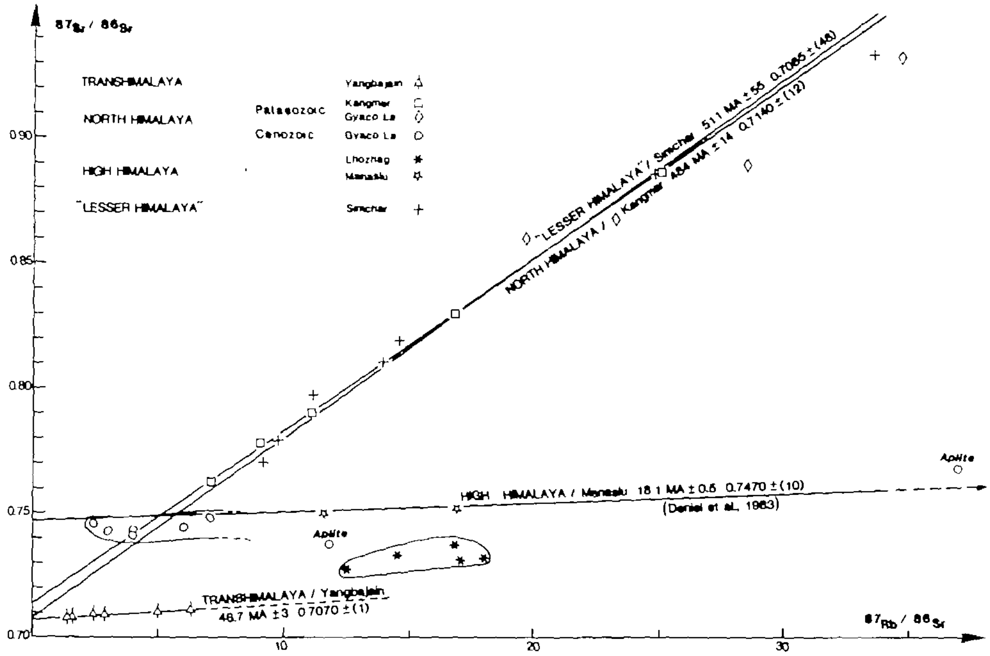

FIG. 12. $^{87}Sr/^{86}Sr$ *vs* $^{87}Rb/^{86}Sr$ diagram for some plutonic units (see Tables 6, 7).

(Fig. 6). Finally, among the Cenozoic granitoids, those of the North Himalaya are usually richer in dark minerals, quartz (Fig. 6) and Ca (Table 3), but poorer in feldspars and alkalis relative to the High Himalaya ones. The North Himalaya granitoids differ by the variability of their dark minerals content and of their muscovite/biotite ratio (Fig. 5), their higher Mg/Fe ratios, and their quartz-rich to quartz-normal associations (Fig. 6). Only the High Himalaya plutons correspond to quartz-poor and very leucocratic associations. Most of these Cenozoic granitoids, however, are typically adamellites, with similar sodic associations, aluminous index and $\delta^{18}O$ values, suggesting that they may be related by a common genetic process. In the same way, the similarities among the different Palaeozoic granitoids (Table 8) suggest that they all originated from another common process.

Chronological data

For the North Himalaya belt, recent chronological data (Tables 6, 7; Fig. 12) have defined both a Lower Palaeozoic ($\simeq$ 485 Ma) and Cenozoic (Eocene) group. The Gyaco La granitic samples lie close to the Kangmar isochron (Fig. 12) and it is very likely that this Lower Ordovician age can be extended to the whole of the 'porphyritic more or less gneissified granite' group. Cenozoic (Eocene) ages refer to both 'two-mica adamellite' plutons and to recrystallized micas of the Lower Ordovician group. No good Rb-Sr whole rock isochron has yet been obtained on this adamellitic group of plutons; 8 samples of the Gyaco La yield only an ill-defined Cenozoic age (Table 7, Fig. 12). Recent K-Ar dates (Debon *et al.*, 1985) lie around 12 Ma, while previous determinations have given ages ranging from 6·5 to 32 Ma (Zhang *et al.*, 1981; Maluski, 1984; Tables 6, 7).

The Rb-Sr isotopic composition of the High Himalaya leucocratic granitoids is very heterogeneous and only recently (Deniel *et al.*, 1983*a*, *b*) has a satisfactory whole rock isochron (giving a Miocene age of $18{\cdot}1 \pm 0{\cdot}5$ Ma) been obtained on 11 out of 17 samples from a hectometric outcrop of the Manaslu pluton (Fig. 12, Table 6). The 5 samples of the Lhozhag pluton do not fall into line on the isochron diagram (Fig. 12, Table 7). Rb-Sr and K-Ar dates on micas or mica-whole rock pairs of the Lhozhag and Manaslu plutons have yielded ages ranging from 13 to 21 Ma (Tables 6, 7). Le Fort (1985) has suggested that the emplacement of the North Himalaya belt seems to be younger than the High Himalaya belt by a few million years.

It is now well established that the age of the 'Lesser Himalaya' plutons is Lower Palaeozoic (e.g. Le Fort *et al.*, 1980, 1983). Several dates on the Simchar and Palung plutons (Table 6) have given ages ranging from 466 to 511 Ma. These results are similar to the age of the porphyritic granite group of the North Himalaya belt ($\simeq$ 485 Ma).

The initial $^{87}Sr/^{86}Sr$ ratios are always high in the Palaeozoic plutons (between 0·708 and more than 0·720) and very high in the Cenozoic ones (mainly between 0·727 and 0·760) (Tables 6 to 8).

Genesis of the three Himalaya belts

South of the Indus-Tsangpo suture there are two groups of aluminous granitoids: a Lower Palaeozoic porphyritic granite group and a Cenozoic equigranular adamellite group.

Lower Palaeozoic group

This group not only includes the 'Lesser Himalaya' belt and North Himalaya Palaeozoic granitoids but also can be equated with the augen gneisses of Formation III in the Tibetan crystalline Slab. In the studied region of the Central Himalaya, Formation III has been followed for nearly 300 km at the base of the Tibetan sedimentary series (see Colchen *et al.*, 1980). It is composed of augen gneisses of high metamorphic grade, with similar geochemical characteristics to the 'Lesser Himalaya' belt (Le Fort, in preparation), and has been dated at 517 ± 62 Ma (2σ) with a high initial Sr isotope ratio of 0·7097 (Le Fort *et al.*, 1982). Thus this Upper Cambrian-Lower Ordovician magmatism occurred on a very large scale, some 10^5 km^2 for the area covered by Fig. 2.

This widespread Lower Palaeozoic magmatism of aluminous character and high $\delta^{18}O$ and initial Sr isotope ratio developed in continental crust which was part of Gondwana at that time. However, the occurrence of numerous microgranular inclusions (Didier, 1973), particularly in 'Lesser Himalaya' plutons, indicates that there is a basic contribution (e.g. Leterrier & Debon, 1978) of presumed mantle origin, despite the relatively high oxygen and strontium isotope ratios of the granites. Being intrusive into sediments of similarly Lower Palaeozoic age, this magmatism must have been emplaced at high crustal levels.

This magmatic event seems to be of epeirogenic rather than of true orogenic nature as no clear evidence has yet been found for Lower Palaeozoic regional metamorphism and severe deformation in the Himalaya. For this reason, it has been suggested by Le Fort *et al.* (1980, 1983) that extensive crustal thinning occurred with simultaneous arching of the crust and the generation of extensive granitic magmas from the heated base of the crust.

The Palaeozoic granitoids have been affected by the Himalayan orogeny in various ways, depending on their localization in the Himalayan belt.

To the south, the 'Lesser Himalaya' plutons belong to the frontal part of the overthrust limb of the MCT. They have been involved in the north-dipping thrust movement, their border zone being orthogneissified and affected by the mesozonal metamorphism (two-micas + garnet) (Le Fort *et al.*, 1983).

To the north, the Palaeozoic granitoids were probably dragged up as caps and xenoliths by the diapirically rising Cenozoic anatectic magmas (Le Fort, 1985). They would thus be strict equivalents of Formation III, the underlying part of the Tibetan Slab being affected by a higher grade of metamorphism and anatexis.

In between, Formation III of the Tibetan Slab has been completely reworked in the ductile shear zone of the MCT and has been affected by the catazonal metamorphism (kyanite to sillimanite) (e.g. Pêcher, 1978). It has become a thin sheet close to the top of the Tibetan Slab.

Cenozoic group

Although a number of minor differences were mentioned above, both the High Himalaya and North Himalaya Cenozoic granitoids have similar chemical and petrological characteristics, ages, and oxygen and strontium isotope ratios. Le Fort (1985) has proposed that they all resulted from a similar anatectic mechanism on comparable source rocks. Thrusting on the Main Central Thrust of a hot Tibetan Slab over slightly metamorphosed Midland formations released fluids that then induced anatexis in the overheated slab with the subsequent generation of a leucocratic adamellite magma (Le Fort, 1975, 1981).

Differences in the characteristics of the Cenozoic North Himalaya and High Himalaya granitoids may be explained by the different structural position of the two belts. In particular, the North Himalaya belt was produced under higher P–T conditions and with a somewhat smaller fluid release. This accounts for its composition being farther away from the eutectic but closer to the composition of the gneissic migmatitic root (e.g. more quartz-rich and less leucocratic).

CONCLUSION

The Transhimalaya belt differs both petrographically and geochemically from the three Himalaya belts to the south. They correspond to two fundamentally distinct suites of cafemic and aluminous types respectively (cf. I- and S-types granitoids, Tu *et al.*, 1981). Three principal periods of magma emplacement have been characterized and these can be related to different geodynamic processes: the Lower Palaeozoic group, with a limited southern extension, was reactivated during the Himalayan orogeny; reactivation of its southern edge explains the localization of the MCT; the Transhimalaya group is linked to the northward subduction of the Tethys ocean floor up to the collision of India and Eurasia; and the Cenozoic Himalaya group is a direct consequence of major continental thrusting that followed the collision.

In the Transhimalaya as a whole, there were two main stages of emplacement. The first one was of Cretaceous age, around 100 Ma, and the second one was Palaeocene-Lower Eocene, around 60 to 45 Ma, more or less marking the time of collision. Between these two phases, there seems to be a gap or at least a more quiescent period with little magmatic activity. One remaining question concerns the reason for reactivation of the system to give the second phase of magmatism. Stratigraphically, Palaeocene-Eocene times mark the end of marine sedimentation; tectonically, nappe emplacement starts after 45 Ma (Mascle, 1985). Thus, the 60–50 Ma period corresponds to the final stage of convergence at the time when flysch sediments from the margins of the two plates could get involved with the subduction process. If this is the case, the water-rich sediments which were dragged along may have enhanced the production of the Transhimalaya magmatism until the movement stopped due to collision.

Unlike the Transhimalaya belt, the Cenozoic granitoid belts cannot be followed westward all the way to northern Pakistan. The High Himalaya belt fades out in the Nanga Parbat region; the North Himalaya reaches the Kailas region (Fig. 1). The western interruptions of the two belts correspond to sharp bends of the frontal part of the Himalaya and of the MCT-MBT trace. This situation may be linked to the former configuration of the two plates with an eastern promontory corresponding to the extension of the North Himalaya belt. For the High Himalaya, the pole of rotation between the Indian and the Eurasian plates lay to the west and therefore the rate of convergence between the two plates decreased from east to west.

ACKNOWLEDGEMENTS

The I.N.A.G. (C.N.R.S.) and Chinese Academy of Geological Sciences (French-Chinese Project on Tibet 1980-82) and the G.R.E.C.O. Himalaya-Karakorum (C.N.R.S.) have supported field work. This field work benefitted from very fruitful collaborations, particularly with Jin Chengwei, Liu Guohue, B. N. Upreti and Xu Ronghua. Laboratory work was supported by the Centre de Recherches Pétrographiques et Géochimiques (C.R.P.G., Nancy). Early drafts of the manuscript were greatly improved by critical comments from G. C. Brown and W. E. Stephens. A. Pêcher and Ph. Vidal are thanked for their help. The technical assistance of P. Coget, D. Dautel, J. Gerbaut, A. Legros and the E.D.T.A. department of the C.R.P.G. is gratefully acknowledged. C.R.P.G. contribution no. 627.

REFERENCES

Academia Sinica, 1980. *A scientific guidebook to South Xizang (Tibet)*. Symp. on Qinghai-Xizang (Tibet) Plateau, Beijing, 104 pp

Afzali, H., Debon, F., Le Fort, P., & Sonet, J., 1979 Le massif monzosyénitique de Zarkachan (Afghanistan central). caractères, âge Rb-Sr et implications tecto-orogéniques. *C.R Acad Sci.*, Paris, **D**, 287-90

Atherton, M. P., McCourt, W. J., Sanderson, L. M., & Taylor, W. P., 1979. The geochemical character of the segmented Peruvian Coastal Batholith and associated volcanics. In: Atherton, M. P. & Tarney, J. (eds.). *Origin of Granite Batholiths. Geochemical evidence* Orpington: Shiva Publ. Ltd , 45-64.

Bertrand, J. M., & Davison, I., 1981. Pan-African granitoid emplacement in the Adrar des Iforas mobile belt (Mali): a Rb/Sr isotope study. *Precambrian Res.* **14**, 333-61.

Besse, J., Courtillot, V., Pozzi, J. P, Westphal, M., & Zhou, Y. X., 1984. Palaeomagnetic estimates of crustal shortening in the Himalayan thrusts and Zangbo suture. *Nature*, **311**, 621-26.

Blattner, P., Dietrich, V., & Gansser, A , 1983 Contrasting ^{18}O enrichment and origins of High Himalayan and Transhimalayan intrusives. *Earth planet. Sci. Lett.* **65**, 276-86.

Brookfield, M. E., & Reynolds, P. H., 1981. Late Cretaceous emplacement of the Indus suture zone ophiolitic mélanges and an Eocene-Oligocene magmatic arc on the northern edge of the Indian plate. *Ibid.* **55**, 157-62.

Brun, J. P., Pons, J., & Wang, F. P., 1983. Sinistral wrenching during pluton emplacement in the Lhasa block (Kangdese batholith, Tibet). *Terra Cognita*, **3**, 264.

Burg, J. P., 1983. Tectogenèse comparée de deux segments de chaine de collision: le Sud du Tibet (suture du Tsangpo)-la chaîne hercynienne en Europe (sutures du Massif Central). *Thèse Sci., Univ. Montpellier, 361 p., one map 1/500 000.*

Chappell, B. W., & White, A. J. R., 1974. Two contrasting granite types *Pacif. Geol.* **8**, 173-4.

Clayton, R. N., & Mayeda, T. K., 1963. The use of bromine pentafluoride in the extraction of oxygen from oxides and silicates for isotopic analysis. *Geochim. cosmochim. Acta*, **27**, 43-52.

Cocherie, A., 1977. Données préliminaires sur la géochimie des terres rares dans le massif leucogranitique du Manaslu (Népal Central). Colloq. int. n°268 '*Ecologie et Géologie de l'Himalaya*', Paris, 1976, Centre Natl. Rech Sci., vol. Sci. de la Terre, 93-110.

Colchen, M., Le Fort, P., & Pêcher, A., 1980. *Carte géologique Annapurna-Manaslu-Ganesh Himalaya du Népal* Echelle: (1.200000). Cent. Natl. Rech. Sci. (éd.), Paris.

Coulon, C., & Wang, S C., 1983. A field study of volcanism from Central and Southern Tibet. *Terra Cognita*, **3**, 265.

Cuney, M., Le Fort, P., & Wang, Z. X., 1984 Uranium and thorium geochemistry and mineralogy in the Manaslu leucogranite (Nepal, Himalaya). In: Xu, K., & Tu, G. (eds.) *Proc Symposium on Geology of granites and their metallogenetic relations.* Nanjing Univ., China, 1982. Beijing Science Press, 853-73.

Debon, F., 1975. *Les massifs granitoïdes à structure concentrique de Cauterets-Panticosa (Pyrénées occidentales) et leurs enclaves. Une étude pétrographique et géochimique. Mém. Sci. de la Terre*, **33**, 420 pp.

—— & Le Fort, P., 1982. A chemical-mineralogical classification of common plutonic rocks and associations. *Trans. R. Soc. Edin.: Earth Sci.* **73**, 135-49.

—— —— & Sonet, J., 1981. Granitoid belts West and South of Tibet About their geochemical trends and Rb-Sr isotopic studies. *Proc. Symp. on Qinghai-Xizang (Tibet) Plateau*, (Beijing, 1980). Beijing: Science Press, New York: Gordon & Breach, **1**, 395-405.

—— Sonet, J., Liu, G. H., Jin, C. W., & Xu, R. H., 1982. Caractères chimico-minéralogiques majeurs et datations par Rb-Sr des trois ceintures plutoniques du Tibet méridional. 1982: *C. R. Acad. Sci.*, Paris, II, 213-18. 1984 In. Mercier, J L., & Li, G. C. (eds) *Mission franco-chinoise au Tibet 1980.* Paris: Cent. Natl. Rech. Sci. 309-17.

——— 1983. Chemical-mineralogical typology and Rb-Sr dating of the three plutonic belts in Southern Tibet. *Terra Cognita*, **3**, 265.

——Zimmermann, J. L., Liu, G. H., Jin, C. W., & Xu, R. H., 1985. Time relationships between magmatism, tectonics and metamorphism in three plutonic belts in southern Tibet: new K-Ar data. *Geol. Rdsch.* **74** (2), 229–36

Deniel, C., Vidal, Ph., & Le Fort, P., 1983*a*. The Manaslu granite (Himalaya, Nepal): new Sr and Nd isotopic data. *Terra cognita*, **3**, 266.

——— 1983*b*. $^{87}Sr/^{86}Sr$ initial heterogeneities in a granitic body: the example of Manaslu leucogranite (Himalaya, Nepal). *EOS Trans. Am. Geophys. Un.* **64**, 18, 337

Didier, J., 1973. *Granites and their enclaves. Developments in Petrology*. Amsterdam: Elsevier, **3**.

Dietrich, V. J, Frank, W., & Honegger, K., 1983. A Jurassic-Cretaceous island arc in the Ladakh-Himalayas. *J. Volcanol. geotherm. Res.*, Spec. issue: *Arc volcanism*, **18**, 405–33.

Evensen, N. M., Hamilton, P. J., & O'Nions, R. K., 1978. Rare-earth abundances in chondritic meteorites. *Geochim. cosmochim. Acta*, **42**, 1199–212.

Fourcade, S., 1981. Géochimie des granitoïdes. *Thèse Sci., Univ. Paris 7*, 189 pp.

——& Allègre, C. J., 1981. Trace elements behavior in granite genesis: a case study. The calc-alkaline plutonic association from the Querigut complex (Pyrénées, France). *Contr. Miner. Petrol.* **76**, 177–95.

Gariepy, C., Xu, R. H., & Allègre, C. J., 1983. Isotopic composition of the granitoid belts of the Himalaya–Tibet area and the genesis of the continental crust. *Terra Cognita*, **3**, 266.

Govindaraju, K., & Mevelle, G., 1983. Geostandards and geochemical analysis. *Spectrochim. Acta*, **38 B**, 1447–56.

———& Chouard, Ch., 1976. Automated optical emission spectrochemical bulk analysis of silicate rocks with microwave plasma excitation. *Analyt. Chem.*, **48**, 1325–31.

Honegger, K., Dietrich, V., Frank, W., Gansser, A., Thöni, M., & Trommsdorff, V., 1982. Magmatism and metamorphism in the Ladakh Himalayas (the Indus-Tsangpo suture zone). *Earth planet. Sci. Lett.* **60**, 253–92.

Jin, C. W., 1981. The Mesozoic-Cenozoic volcanic rocks in Xizang and their bearing on geology. *Proc. symp. on Qinghai-Xizang (Tibet) Plateau (Beijing, 1980)*, **1**, Beijing Science Press, New York: Gordon & Breach, 433–42.

——& Xu, R. H., 1984. Les granitoïdes de la partie centrale de l'Himalaya et du Gangdise au Xizang (Tibet) méridional In: Mercier, J. L., & Li, G. C. (eds.) *Mission franco-chinoise au Tibet 1980*. Paris: Cent. Natl. Rech Sci. 289–308.

Kuno, H., 1968. Differentiation of basalt magmas. In: Hess, H. H., & Poldervaart, A. (eds.) *Basalts. The Poldervaart Treatise on rocks of basaltic composition*. New York: Interscience Publ., 623–88.

La Roche, H. de, 1964. Sur l'expression graphique des relations entre la composition chimique et la composition minéralogique quantitative des roches cristallines. Présentation d'un diagramme destiné à l'étude chimico-minéralogique des massifs granitiques ou grano-dioritiques. Application aux Vosges cristallines. *Sci. de la Terre*, **9**, 293–337.

——1966. Sur l'usage du concept d'association minérale dans l'étude chimique des roches: modèles chimiques, statistiques, représentations graphiques, classification chimico-minéralogique. *C. R. Acad. Sci.* Paris, **262 D**, 1665–8.

——1980. Granites' chemistry through multicationic diagrams. *Sci. de la Terre, Inf. Géol.* **13**, 65–88.

——Stussi, J. M., & Chauris, L., 1980. Les granites à deux micas hercyniens français. Essais de cartographie et de corrélations géochimiques appuyés sur une banque de données. Implications pétrologiques et métallogéniques. *Sci. de la Terre*, **24**, 5–121.

Le Fort, P., 1973. Les leucogranites à tourmaline de l'Himalaya sur l'exemple du granite du Manaslu (Népal central). *Bull. Soc. géol. Fr.* (7), **XV**, 555–61.

——1975. Himalaya: the collided range. Present knowledge of the continental arc. *Am. J. Sci.* **275-A**, 1–44

——1981. Manaslu leucogranite: a collision signature of the Himalaya. A model for its genesis and emplacement. *J Geophys. Res.*, **86B**, 10545–68.

——1985. Metamorphism and magmatism during the Himalayan collision. *William Smith Lecture*, London, 1983, Geol. Soc. London, in press.

——Debon, F., & Sonet, J., 1980. The 'Lesser Himalayan' cordierite granite belt. Typology and age of the pluton of Manserah (Pakistan) *Geol Bull. Univ. Peshawar, Spec. Issue*, **13**, 51–61.

——— 1983. The Lower Paleozoic 'Lesser Himalayan' granitic belt: emphasis on the Simchar pluton of Central Nepal. In: Shams, F. A. (ed.) *Granites of Himalayas Karakorum and Hindu Kush*. Lahore: Punjab University, 235–55.

——Pêcher, A., & Vidal, Ph., 1982. Les gneiss oeillés de la Dalle du Tibet: un épisode magmatique au Paléozoïque inférieur en Himalaya du Népal. *9è Réunion ann. Sci. de la Terre*, Paris, Soc. géol. Fr. (éd.), 369.

Le Maitre, R. W., 1976 The chemical variability of some common igneous rocks. *J. Petrology*, **17**, 589–637.

Leterrier, J., 1972. *Etude pétrographique et géochimique du massif granitique de Quérigut (Ariège)*. Mém. Sci. de la Terre, **23**, 292 pp.

——& Debon, F., 1978. Caractères chimiques comparés des roches granitoïdes et de leurs enclaves microgrenues. Implications génétiques. *Bull. Soc. géol. Fr.* **20**, 3–10.

Liu, G. H., 1984. Les caractéristiques et la genèse des ceintures granitiques au Sud du Tibet. In: Mercier, J. L., & Li, G. C. (eds.). *Mission franco-chinoise au Tibet 1980*. Paris, Cent. Natl. Rech. Sci., 255–87.

Maluski, H., 1984. ^{39}Ar–^{40}Ar ages of some granitic bodies and metamorphic series of the North Himalayan belt (Southern Tibet-China). In: *Int. Symp. on Geology of the Himalayas*, June 5–11, Chengdu, China, Abstr. **2**, 43.

Maluski, H., Proust, F., & Xiao, X. C., 1982. $^{39}Ar/^{40}Ar$ dating of the trans-Himalayan calc-alkaline magmatism of Southern Tibet *Nature*, **298**, 152-4.

Mascle, G., 1985. L'Himalaya résulte-t-il du télescopage de trois chaines? *Bull. Soc. géol. Fr.* **3**, 289-304.

Mitchell, A. H. G., 1981. Himalayan and Transhimalayan granitic rocks in and adjacent to Nepal and their mineral potential. *J. Nepal geol. Soc.* **1**, 41-52.

Pagel, M., & Leterrier, J., 1980. The subalkaline potassic magmatism of the Ballons massif (Southern Vosges, France): shoshonitic affinities. *Lithos*, **13**, 1-10.

Patriat, Ph., & Achache, J., 1984 India-Eurasia collision chronology has implications for crustal shortening and driving mechanism of plates *Nature*, **311**, 615-21.

Pêcher, A., 1978. Déformations et métamorphisme associés à une zone de cisaillement. Exemple du grand chevauchement central himalayen (M.C.T.), transversale des Annapurnas et du Manaslu, Népal *Thèse Sci., Grenoble*, 354 p.

Pitcher, W. S., 1978. The anatomy of a batholith *J. geol. Soc. Lond.* **135**, 157-82.

Proust, F., Burg, J. P., Matte, Ph., Tapponnier, P., Li, T. D., Li, G. C., & Chen, G. M., 1984. Succession des phases de plissement sur une transversale du Tibet méridional, implications géodynamiques. In: Mercier, J. L., & Li, G. C. (eds.) *Mission franco-chinoise au Tibet 1980*. Paris. Cent. Natl. Rech. Sci., 385-92

Reibel, G., & Juteau, T., 1981. Les volcanites de la formation de Dras, suture de l'Indus (Ladakh), des tholéiites océaniques aux tholéiites d'arc. *C. R. Acad. Sci.* Paris, **293**, II, 57-60.

Schärer, U., & Allègre, C. J., 1983. The Palung granite (Himalaya): high-resolution U-Pb systematics in zircon and monazite. *Earth planet. Sci. Lett.* **63**, 423-32.

—— Hamet, J., & Allègre, C. J., 1984*a*. The Transhimalaya (Gangdese) plutonism in the Ladakh region: a U-Pb and Rb-Sr study. *Ibid.* **67**, 327-39.

——Xu, R. H., & Allègre, C. J., 1984*b*. U-Pb geochronology of Gangdese (Transhimalaya) plutonism in the Lhasa-Xigaze region, Tibet. *Ibid.* **69**, 311-20

Sheppard, S. M F., Debon, F., Liu, G. H., Jin, C. W., & Xu, R. H., 1983. Oxygen isotope relationships in three plutonic belts in Southern Tibet. *Terra Cognita*, **3**, 272.

Streckeisen, A. L., 1976. To each plutonic rock its proper name. *Earth Sci. Rev.* **12**, 1-33.

Taylor, H. P., 1968. The oxygen isotope geochemistry of igneous rocks. *Contr. Miner. Petrol.* **19**, 1-71.

Trommsdorff, V., Dietrich, V., & Honegger, K., 1982. The Indus suture zone: paleotectonic and igneous evolution in the Ladakh-Himalayas. In: Hsü, K. J. (ed.) *Mountain building processes*. Academic Press, 215-19.

Tu, G. Z., Zhang, Y. Q., Zhao, Z. H., & Wang, Z. G., 1981. Characteristic and evolution of granitoids of Southern Xizang. *Proc. Symp. on Qinghai-Xizang (Tibet) Plateau*, (Beijing, 1980). **1**, Beijing: Science Press; New York: Gordon & Breach, 353-61.

—— —— & Wang, Z. G., 1982. *Geochemistry of granitoid rocks in Southern Xizang* (in Chinese). Beijing: Science Press.

Vidal, Ph., Cocherie, A., & Le Fort, P., 1982. Geochemical investigations of the origin of the Manaslu leucogranite (Himalaya, Nepal). *Geochim, cosmochim. Acta*, **46**, 2279-92.

—— Bernard-Griffiths, J., Cocherie, A., Le Fort, P., Peucat, J. J., & Sheppard, S. M. F, 1984. Geochemical comparison between Himalayan and Hercynian leucogranites. *Phys. Earth planet. Interiors* Spec. issue, **35**, 179-90.

Wang, J. W., Chen, Z L., Gui, X. T., Xu, R H., & Zhang, Y. Q., 1981. Rb-Sr isotope studies on some intermediate-acid plutons in Southern Xizang. *Proc. Symp. on Qinghai-Xizang (Tibet) Plateau*, (Beijing, 1980), Beijing: Science Press; New York: Gordon & Breach, **1**, 515-20.

Westphal, M., Pozzi, J. P., & Zhou, Y. X., 1982. Motion in latitude of the Lhasa block during Late Cretaceous-Early Tertiary. *EOS Trans Am. geophys. Un.* **63**, 45, 1093.

Xu, R. H., Schärer, U., & Allègre, C. J., 1982. Timing of the Tibetan collision by radiometric dating. *Ibid.* **63**, 45, 1094.

—— —— —— 1985. Magmatism and metamorphism in the Lhasa block (Tibet): a geochronological study. *J Geol.* **93**, 41-57.

Zhang, Y. Q., Dai, T. M., & Hong, A. S., 1981 Isotopic geochronology of granitoid rocks in southern Xizang Plateau. *Proc. Symp. on Qinghai-Xizang (Tibet) Plateau*, (Beijing, 1980), **1**, Beijing: Science Press; New York: Gordon & Breach, 483-95.

Zhou, Y. S., & Jin, C. W., 1983. Plutonism and its tectonic environment in the Gangdese and Nyainqentanglha mountains of Xizang, China. In: Shams, F. A. (ed.) *Granites of Himalayas, Karakorum and Hindu Kush*. Lahore: Punjab University, 393-406.